INTERNATIONAL JOURNAL OF
NUMERICAL ANALYSIS AND MODELING
Volume 21, Number 1, Pages 65–103

doi: 10.4208/ijnam2024-1003

A POSTERIORI ERROR ESTIMATES FOR DARCY-FORCHHEIMER'S PROBLEM COUPLED WITH THE CONVECTION-DIFFUSION-REACTION EQUATION

FAOUZI TRIKI, TONI SAYAH*, AND GEORGES SEMAAN

Abstract. In this work we derive *a posteriori* error estimates for the convection-diffusion-reaction equation coupled with the Darcy-Forchheimer problem by a nonlinear external source depending on the concentration of the fluid. We introduce the variational formulation associated to the problem, and discretize it by using the finite element method. We prove optimal *a posteriori* errors with two types of calculable error indicators. The first one is linked to the linearization and the second one to the discretization. Then we find upper and lower error bounds under additional regularity assumptions on the exact solutions. Finally, numerical computations are performed to show the effectiveness of the obtained error indicators.

Key words. Darcy-Forchheimer problem, convection-diffusion-reaction equation, finite element method, *a posteriori* error estimates.

1. Introduction.

This work deals with the *a posteriori* error estimate of the Darcy-Forccheimer system coupled with the convection-diffusion-reaction equation. We consider following system of equations:

$$(P)\left\{\begin{array}{rcll} \dfrac{\mu}{\rho}K^{-1}\mathbf{u}+\dfrac{\beta}{\rho}|\mathbf{u}|\mathbf{u}+\nabla p &=& \mathbf{f}(\cdot,C) & \text{in}\,\Omega,\\ \operatorname{div}\mathbf{u} &=& 0 & \text{in}\,\Omega,\\ -\alpha\Delta C+\mathbf{u}\cdot\nabla C+r_0C &=& g & \text{in}\,\Omega,\\ \mathbf{u}\cdot\mathbf{n} &=& 0 & \text{on}\,\Gamma,\\ C &=& 0 & \text{on}\,\Gamma, \end{array}\right.$$

where $\Omega \subset \mathbb{R}^d$, $d = 2, 3$, is a bounded simply-connected open domain, having a Lipschitz-continuous boundary Γ with an outer unit normal $\mathbf{n}$. The unknowns are the velocity $\mathbf{u}$, the pressure p and the concentration C of the fluid. $|.|$ denotes the Euclidean norm, $|\mathbf{u}|^2 = \mathbf{u}\cdot\mathbf{u}$. The parameters ρ, μ and β represent the density of the fluid, its viscosity and its dynamic viscosity, respectively. β is also referred as Forchheimer number when it is a scalar positive constant. The diffusion coefficient α and the parameter r_0 are strictly positive constants. The function $\mathbf{f}$ represents an external force that depends on the concentration C and the function g represents an external concentration source. K is the permeability tensor, assumed to be uniformly positive definite (i.e $x^TKx > 0$ for all $x \in R^d \setminus \{\mathbf{0}\}$) and bounded such that there exist two positive real numbers K_m and K_M such that

$$0 < K_m \le \left\|K^{-1}\right\|_{L^\infty(\Omega)^{d\times d}} \le K_M. \tag{1}$$

It is important to note that K_m should be smaller than the smallest eigenvalue of K^{-1} over Ω and K_M could be very large.

Received by the editors June 14, 2022 and, accepted on October 3, 2023.
2000 *Mathematics Subject Classification.* 35K05, 65N30, 65N15, 65M15, 65M50.
*Corresponding author.

System (P) represents the coupling of the Darcy-Forchheimer problem with the convection-diffusion-reaction equation satisfied by the concentration of the fluid. The same system can represent the coupling of the Darcy-Forchheimer system with the heat equation by replacing the concentration C by the temperature T and setting $r_0 = 0$.

Darcy's law (see [31] and [42] for the theoretical derivation) is an equation that describes the flow of a fluid through a porous medium. This law was formulated by Darcy based on experimental results. It is simply the first equation of the system (P) where the dynamic viscosity $\beta = 0$. In the case where the velocity of the fluid is higher and the porosity is non uniform, Forchheimer proposed the Darcy-Forchheimer equation (see [22]) which is the first equation of system (P) by adding the non-linear term). Several numerical and theoretical studies of the Darcy-Forchheimer equation were performed, and among others we mention [25, 27, 32, 28, 33].

For the coupling of Darcy's equation with the heat equation, we refer to [9] where the system is treated using a spectral method. The authors in [7] and [16] considered the same stationary system but coupled with a nonlinear viscosity that depends on the temperature. In [17], the authors derived an optimal *a posteriori* error estimate for each of the numerical schemes proposed in [7]. We can also refer to [3] where the authors used a vertex-centred finite volume method to discretize the coupled system. For physical applications of system (P), we refer to [39]. In [36], we introduced the variational formulation associated to system (P), and we showed uniqueness under additional constraints on the concentration. Then, we discretized the system by using the finite element method and we showed the existence and uniqueness of corresponding solutions. Moreover, we established the *a priori* error estimate between the exact and numerical solutions and introduced a numerical scheme where we studied the corresponding convergence.

I. Babuška was the first who introduced *a posteriori* analysis (see [4]), then it was developed by R. Verfürth [41], and has been the object of a large number of publications. Many works have established the *a posteriori* error estimates for the Darcy flow, see for instance [2, 10, 11, 29]. In [17], the authors established *a posteriori* error estimates for Darcy's problem coupled with the heat equation. Sayah T. (see [34]) established the *a posteriori* error estimates for the Brinkman-Darcy-Forchheimer problem. Moreover, in [35], we established the *a posteriori* estimates for the Darcy-Forchheimer problem without the convection-diffusion-reaction equation. Furthermore, several works established the *a priori* and *a posteriori* errors for the time-dependent convection-diffusion-reaction equation coupled with Darcy's equation(see [12, 13]).

The main goal of this work is to derive the *a posteriori* error estimates associated to the coupling system (P) for the numerical scheme introduced in [36]. We start by recalling some auxiliary results from [36] concerning the discretization of system (P), and the numerical scheme with the corresponding convergence. In a second step, we establish the *a posteriori* error estimates where the error between the exact and iterative numerical solutions are bounded by two types of local indicators: the indicators of discretization and the indicators of linearization. Then, we show the corresponding efficiency by bounding each indicator by the local error. Finally, we present some numerical computations in order to show the effectiveness of the proposed method.

The outline of the paper is as follows:

- Section 2 is devoted to the continuous problem.

- In section 3, we introduce the discrete and iterative problems and recall their main properties.
- In section 4, we provide the error indicators and prove the upper and lower error bounds.
- Numerical results validating the theory are presented in section 5.

We further assume that the volumic and boundary sources satisfy the following conditions:

Assumption 1.1. *The functions* $\mathbf{f}$ *and* g *satisfy:*

(1) $\mathbf{f}$ *can be written as follows:*

$$\forall \mathbf{x} \in \Omega, \forall C \in \mathbb{R}, \qquad \mathbf{f}(\mathbf{x}, C) = \mathbf{f}_0(\mathbf{x}) + \mathbf{f}_1(C), \tag{2}$$

where $\mathbf{f}_0 \in L^{\frac{3}{2}}(\Omega)^d$ *and* $\mathbf{f}_1$ *is Lipschitz-continuous with constant* $c_{\mathbf{f}_1} > 0$*, and verifies* $\mathbf{f}_1(0) = 0$*. In particular we have*

$$\forall \xi \in \mathbb{R},\ |\mathbf{f}_1(\xi)| \leq c_{\mathbf{f}_1} |\xi|,$$

(2) $g \in L^2(\Omega)$*.*

Remark 1.2. *The decomposition of the source term* $\mathbf{f}(x, C) = \mathbf{f}_0(\mathbf{x}) + \mathbf{f}_1(C)$ *in the coupling of the Darcy-Forchheimer model with the concentration equation (or heat equation with* $r_0 = 0$*) has physical explanations that can be related to real situations involving fluid flow and concentration transfer (or heat transfer). Indeed the term* $\mathbf{f}_0(\mathbf{x})$ *represents the source contribution related to fluid flow through porous media (modeled by the Darcy-Forchheimer equation), and the term* $\mathbf{f}_1(C)$ *represents the impact of the concentration on the source term. Therefore, the separation of the source term simplifies the treatment and the study of the considered coupling system.*

2. Variational Formulation

In order to introduce the variational formulation, we recall some classical Sobolev spaces and their properties. Let $\mathbf{x} = (x_1, x_2, \ldots, x_d) \in \mathbb{R}^d$, and let $\alpha = (\alpha_1, \alpha_2, \ldots, \alpha_d)$ be a vector of non negative integers, set $|\alpha| = \sum_{i=1}^d \alpha_i$, and define the partial derivative ∂^α by

$$\partial^\alpha = \frac{\partial^{|\alpha|}}{\partial x_1^{\alpha_1} \partial x_2^{\alpha_2} \ldots \partial x_d^{\alpha_d}}.$$

Then, for any positive integer m and number $p \geq 1$, we recall the classical Sobolev space [1, 30]

$$W^{m,p}(\Omega) = \{v \in L^p(\Omega);\ \forall\, |\alpha| \leq m,\ \partial^\alpha v \in L^p(\Omega)\}, \tag{3}$$

equipped with the seminorm

$$|v|_{W^{m,p}(\Omega)} = \Big(\sum_{|\alpha|=m} \int_\Omega |\partial^\alpha v|^p \, d\mathbf{x} \Big)^{\frac{1}{p}} \tag{4}$$

and the norm

$$\|v\|_{W^{m,p}(\Omega)} = \Big(\sum_{0 \leq k \leq m} |v|^p_{W^{k,p}(\Omega)} \Big)^{\frac{1}{p}}. \tag{5}$$

When $p = 2$, this space is the Hilbert space $H^m(\Omega)$. The definitions of these spaces are extended straightforwardly to vectors, with the same notation, but with the following modification for the norms in the non-Hilbert case. Let $\mathbf{v}$ be a vector valued function; we set

$$\|\mathbf{v}\|_{L^p(\Omega)^d} = \Big(\int_\Omega |\mathbf{v}|^p \, d\mathbf{x} \Big)^{\frac{1}{p}}, \tag{6}$$

where $|.|$ denotes the Euclidean vector norm.

For vanishing boundary values, we define

$$
\begin{aligned}
H_0^1(\Omega) =& \{v \in H^1(\Omega);\ v_{|\Gamma} = 0\},\\
W_0^{1,q}(\Omega) =& \{v \in W^{1,q}(\Omega);\ v_{|\Gamma} = 0\}.
\end{aligned}
\tag{7}
$$

We shall often use the following Sobolev embeddings: for any real number $p \geq 1$ when $d = 2$, or $1 \leq p \leq \frac{2\,d}{d-2}$ when $d \geq 3$, there exist constants S_p and S_p^0 such that

$$
\forall\, v \in H^1(\Omega),\ \|v\|_{L^p(\Omega)} \leq S_p \|v\|_{H^1(\Omega)}
\tag{8}
$$

and

$$
\forall\, v \in H_0^1(\Omega),\ \|v\|_{L^p(\Omega)} \leq S_p^0 |v|_{H^1(\Omega)}.
\tag{9}
$$

When $p = 2$, (9) reduces to Poincaré's inequality.

To deal with the Darcy-Forchheimer, we recall the space

$$
L_0^2(\Omega) = \big\{v \in L^2(\Omega);\ \int_\Omega v\, d\mathbf{x} = 0\big\}.
\tag{10}
$$

It follows from the nonlinear term in the system (P) that the velocity $\mathbf{u}$ and the test function $\mathbf{v}$ must belong to $L^3(\Omega)^d$; then, the gradient of the pressure must belong to $L^{\frac{3}{2}}(\Omega)^d$. Furthermore, the concentration C must be in $H_0^1(\Omega)$. Thus, we introduce the spaces (see [25])

$$
X = L^3(\Omega)^d, \quad M = W^{1,\frac{3}{2}}(\Omega) \cap L_0^2(\Omega), \quad Y = H_0^1(\Omega).
$$

Furthermore, we recall the following inf-sup condition between X and M (see [25]),

$$
\inf_{q \in M} \sup_{\mathbf{v} \in X} \frac{\displaystyle\int_\Omega \mathbf{v}(\mathbf{x}) \cdot \nabla q(\mathbf{x})\, d\mathbf{x}}{\|\mathbf{v}\|_{L^3(\Omega)^d}\, \|\nabla q\|_{L^{\frac{3}{2}}(\Omega)}} = 1.
\tag{11}
$$

We introduce the following variational formulation associated to problem (P):

$$
(V_a)\begin{cases}
\text{Find } (\mathbf{u}, p, C) \in X \times M \times Y \text{ such that:}\\
\forall \mathbf{v} \in X,\ \dfrac{\mu}{\rho} \displaystyle\int_\Omega (K^{-1}\mathbf{u}(\mathbf{x})) \cdot \mathbf{v}(\mathbf{x})\, d\mathbf{x} + \dfrac{\beta}{\rho} \int_\Omega |\mathbf{u}(\mathbf{x})| \mathbf{u}(\mathbf{x}) \cdot \mathbf{v}(\mathbf{x})\, d\mathbf{x}\\
\qquad + \displaystyle\int_\Omega \nabla p(\mathbf{x}) \cdot \mathbf{v}(\mathbf{x})\, d\mathbf{x} = \int_\Omega \mathbf{f}(\mathbf{x}, C(\mathbf{x})) \cdot \mathbf{v}(\mathbf{x})\, d\mathbf{x},\\
\forall q \in M,\ \displaystyle\int_\Omega \nabla q(\mathbf{x}) \cdot \mathbf{u}(\mathbf{x})\, d\mathbf{x} = 0,\\
\forall S \in Y,\ \alpha \displaystyle\int_\Omega \nabla C(\mathbf{x}) \cdot \nabla S(\mathbf{x})\, d\mathbf{x} + \int_\Omega (\mathbf{u} \cdot \nabla C)(\mathbf{x}) S(\mathbf{x})\, d\mathbf{x}\\
\qquad + r_0 \displaystyle\int_\Omega C(\mathbf{x}) S(\mathbf{x})\, d\mathbf{x} = \int_\Omega g(\mathbf{x}) S(\mathbf{x})\, d\mathbf{x}.
\end{cases}
$$

The existence and uniqueness of the solutions to the problem (V_a) can be found in [36]. To study the discretization of the variational problem (V_a), it is convenient to introduce the nonlinear mapping:

$$
\begin{aligned}
\mathcal{A}:\ & L^3(\Omega)^d && \mapsto\ L^{\frac{3}{2}}(\Omega)^d\\
& \mathbf{v} && \mapsto\ \mathcal{A}(\mathbf{v}) = \frac{\mu}{\rho} K^{-1}\mathbf{v} + \frac{\beta}{\rho} |\mathbf{v}| \mathbf{v}.
\end{aligned}
$$

We refer to [25, 21] for the following useful results.

Property 2.1. *$\mathcal{A}$ satisfies the following properties:*

(1) *$\mathcal{A}$ maps $L^3(\Omega)^d$ into $L^{\frac{3}{2}}(\Omega)^d$ and we have for all $\mathbf{v} \in L^3(\Omega)^d$:*

$$\|\mathcal{A}(\mathbf{v})\|_{L^{\frac{3}{2}}(\Omega)^d} \leq \frac{\mu}{\rho} \left\|K^{-1}\right\|_\infty \|\mathbf{v}\|_{L^{\frac{3}{2}}(\Omega)^d} + \frac{\beta}{\rho} \|\mathbf{v}\|^2_{L^3(\Omega)^d}.$$

(2) *For all $(\mathbf{v}, \mathbf{w}) \in \mathbb{R}^d \times \mathbb{R}^d$, we have,*

$$|\mathcal{A}(\mathbf{v}) - \mathcal{A}(\mathbf{w})| \leq \left(\frac{\mu}{\rho} \left\|K^{-1}\right\|_\infty + \frac{\beta}{\rho}(|\mathbf{v}| + |\mathbf{w}|) \right) |\mathbf{v} - \mathbf{w}|. \tag{12}$$

(3) *$\mathcal{A}$ is monotone from $L^3(\Omega)^d$ into $L^{\frac{3}{2}}(\Omega)^d$, and we have for all $\mathbf{v}, \mathbf{w} \in L^3(\Omega)^d$,*

$$\begin{aligned} &\int_\Omega (\mathcal{A}(\mathbf{v}(\mathbf{x})) - \mathcal{A}(\mathbf{w}(\mathbf{x}))) \cdot (\mathbf{v}(\mathbf{x}) - \mathbf{w}(\mathbf{x}))\, d\mathbf{x} \\ &\geq \max(c_m \|\mathbf{v} - \mathbf{w}\|^3_{L^3(\Omega)^d}, \frac{\mu}{\rho} K_m \|\mathbf{v} - \mathbf{w}\|^2_{L^2(\Omega)^d}), \end{aligned} \tag{13}$$

where c_m is a strictly positive constant.

(4) *$\mathcal{A}$ is coercive in $L^3(\Omega)^d$:*

$$\lim_{\|\mathbf{u}\|_{L^3(\Omega)^d} \to \infty} \frac{\displaystyle\int_\Omega \mathcal{A}(\mathbf{u}) \cdot \mathbf{u}\, d\mathbf{x}}{\|\mathbf{u}\|_{L^3(\Omega)^d}} = +\infty.$$

(5) *$\mathcal{A}$ is hemi-continuous in $L^3(\Omega)^d$: for fixed $\mathbf{u}, \mathbf{v} \in L^3(\Omega)^d$, the mapping*

$$t \longrightarrow \int_\Omega \mathcal{A}(\mathbf{u} + t\mathbf{v}) \cdot \mathbf{v}\, d\mathbf{x}$$

is continuous from $\mathbb{R}$ into $\mathbb{R}$.

3. Discretization

In this section, we recall the discretization of problem (P) introduced in [36], and restrict the analysis to dimensions $d = 2, 3$. We begin by introducing a nonlinear discrete problem associated to (P) and then we recall the corresponding properties (bounds of the discrete solution, *a priori* error estimate, ...). Next, we introduce an iterative problem in order to approximate the solution of the nonlinear discrete problem and to establish the corresponding bound and convergence under some assumptions.

We assume that Ω is a polygon when $d = 2$ or polyhedron when $d = 3$, so it can be completely meshed. Next, we describe the space discretization. A regular family of triangulations (see Ciarlet [14]) $(\mathcal{T}_h)_h$ of Ω, is a set of closed non degenerate triangles for $d = 2$ or tetrahedra for $d = 3$, called elements, satisfying

- for each h, $\bar{\Omega}$ is the union of all elements of $\mathcal{T}_h$;
- the intersection of two distinct elements of $\mathcal{T}_h$ is either empty, a common vertex, or an entire common edge (or face when $d = 3$);
- the ratio of the diameter h_κ of an element $\kappa \in \mathcal{T}_h$ to the diameter ρ_κ of its inscribed circle when $d = 2$ or ball when $d = 3$ is bounded by a constant independent of h, that is, there exists a strictly positive constant σ independent of h such that,

$$\max_{\kappa \in \mathcal{T}_h} \frac{h_\kappa}{\rho_\kappa} \leq \sigma. \tag{14}$$

As usual, h denotes the maximal diameter of all elements of $\mathcal{T}_h$. To define the finite element functions, let r be a non negative integer. For each κ in $\mathcal{T}_h$, we denote by $\mathbb{P}_r(\kappa)$ the space of restrictions to κ of polynomials in d variables and total degree at most r, with a similar notation on the faces or edges of κ. For every edge (when $d = 2$) or face (when $d = 3$) e of the mesh $\mathcal{T}_h$, we denote by h_e the diameter of e.

In order to use inverse inequalities, we assume that the family or triangulations is uniformly regular in the following sense: there exists $\beta_0 > 0$ such that, for every element $\kappa \in \mathcal{T}_h$, we have

$$h_\kappa \geq \beta_0 h. \tag{15}$$

We shall use the following inverse inequality: for any numbers $p, q \geq 2$, for any dimension d, and for any non negative integer r, there exist constants $c_I(p) > 0$, $c_J(q) > 0$, and $c_L > 0$ such that for any polynomial function v_h of degree r on an element κ or an edge (when $d = 2$) or face (when $d = 3$) e of the mesh $\mathcal{T}_h$,

$$\begin{aligned} \|v_h\|_{L^p(\kappa)} &\leq c_I(p) h_\kappa^{\frac{d}{p}-\frac{d}{2}} \|v_h\|_{L^2(\kappa)}, \\ \|v_h\|_{L^q(e)} &\leq c_J(q) h_e^{\frac{d-1}{q}-\frac{d-1}{2}} \|v_h\|_{L^2(e)}, \\ |v_h|_{H^1(\kappa)} &\leq c_L h_\kappa^{\frac{d}{2}-\frac{d}{p}-1} \|v_h\|_{L^p(\kappa)}, \end{aligned} \tag{16}$$

where c_I, c_J and c_L depend on the regularity parameter σ of (14).

Let $X_h \subset X$, $M_h \subset M$ and $Y_h \subset Y$ be the discrete spaces corresponding to the velocity, the pressure and the concentration. In the following section we will give the explicit form of these spaces and introduce a nonlinear discrete problem.

3.1. Discrete Scheme. We recall the discrete problem introduced in [36]: Find $(\mathbf{u}_h, p_h, C_h) \in X_h \times M_h \times Y_h$ such that

(17)

$$(V_{ah}) \begin{cases} \forall \mathbf{v}_h \in X_h, & \displaystyle\int_\Omega \mathcal{A}(\mathbf{u}_h) \cdot \mathbf{v}_h d\mathbf{x} + \int_\Omega \nabla p_h \cdot \mathbf{v}_h \, d\mathbf{x} = \int_\Omega \mathbf{f}(C_h) \cdot \mathbf{v}_h \, d\mathbf{x}, \\ \forall q_h \in M_h, & \displaystyle\int_\Omega \nabla q_h \cdot \mathbf{u}_h \, d\mathbf{x} = 0, \\ \forall S_h \in Y_h, & \alpha \displaystyle\int_\Omega \nabla C_h \cdot \nabla S_h \, d\mathbf{x} + \int_\Omega (\mathbf{u}_h \cdot \nabla C_h) S_h \, d\mathbf{x} \\ & \quad + \displaystyle\frac{1}{2} \int_\Omega \operatorname{div}(\mathbf{u}_h) \, C_h S_h d\mathbf{x} + r_0 \int_\Omega C_h S_h \, d\mathbf{x} = \int_\Omega g S_h \, d\mathbf{x}. \end{cases}$$

In the following, we will introduce the finite dimension spaces X_h, M_h and Y_h. Let κ be an element of $\mathcal{T}_h$ with vertices a_i, $1 \leq i \leq d+1$, and corresponding barycentric coordinates λ_i. We denote by $b_\kappa \in \mathbb{P}_{d+1}(\kappa)$ the basic bubble function :

$$b_\kappa(\mathbf{x}) = \lambda_1(\mathbf{x}) \ldots \lambda_{d+1}(\mathbf{x}). \tag{18}$$

We observe that $b_\kappa(\mathbf{x}) = 0$ on $\partial\kappa$ and that $b_\kappa(\mathbf{x}) > 0$ in the interior of κ.
We introduce the following discrete spaces:

$$\begin{aligned} X_h &= \{\mathbf{v}_h \in (\mathcal{C}^0(\bar{\Omega}))^d;\ \forall \kappa \in \mathcal{T}_h,\ \mathbf{v}_h|_\kappa \in \mathcal{P}(\kappa)^d\}, \\ M_h &= \{q_h \in C^0(\bar{\Omega});\ \forall \kappa \in \mathcal{T}_h,\ q_h|_\kappa \in \mathbb{P}_1(\kappa)\} \cap L^2_0(\Omega), \\ Y_h &= \{q_h \in C^0(\bar{\Omega});\ \forall \kappa \in \mathcal{T}_h,\ q_h|_\kappa \in \mathbb{P}_1(\kappa)\} \cap H^1_0(\Omega), \\ V_h &= \{\mathbf{v}_h \in X_h; \forall q_h \in M_h, \int_\Omega \nabla q_h \cdot \mathbf{v}_h \, d\mathbf{x} = 0\}, \end{aligned} \tag{19}$$

where

$$\mathcal{P}(\kappa) = \mathbb{P}_1(\kappa) \oplus \operatorname{Vect}\{b_\kappa\}.$$

In this case, the following inf-sup condition holds [24]:

$$\forall\, q_h \in M_h,\ \sup_{\mathbf{v}_h\in X_h} \frac{\displaystyle\int_\Omega \nabla q_h \cdot \mathbf{v}_h\, d\mathbf{x}}{\|\mathbf{v}_h\|_{X_h}} \geq \beta_2 \|q_h\|_{M_h}, \tag{20}$$

where β_2 is a strictly positive constant independent of h.
The existence and uniqueness of solutions of problem (V_{ah}) can be deduced from inf-sup condition (20) (see for instance [36]).

In order to recall the *a priori* error estimates and establish later the *a posteriori* error bounds, we will introduce some projection operators. We shall use the following results (see [36] and [35]):

(1) For the concentration: there exists an approximation operator (when $d = 2$, see Bernardi and Girault [8] or Clément [15]; when $d = 2$ or $d = 3$, see Scott and Zhang [38]), R_h in the space of linear continous operators from $W^{1,p}(\Omega)$ to Y_h, $\mathcal{L}(W^{1,p}(\Omega); Y_h)$, such that for all κ in $\mathcal{T}_h$, $m = 0, 1$, $l = 0, 1$, and all $p \geq 1$,

$$\forall\, S \in W^{l+1,p}(\Omega),\ |S - R_h(S)|_{W^{m,p}(\kappa)} \leq c(p, m, l)\, h^{l+1-m} |S|_{W^{l+1,p}(\Delta_\kappa)}, \tag{21}$$

where Δ_κ is the macro element containing the values of S used in defining $R_h(S)$. Furthermore for all κ in $\mathcal{T}_h$, for all e in $\partial\kappa$ and for all $S \in H^1(\Omega)$,

$$\|S - R_h S\|_{L^2(e)} \leq c_e h_e^{1/2} |S|_{H^1(w_e)}, \tag{22}$$

where $c_e > 0$ is a positive constant independent of h and w_e is the union of elements of $\mathcal{T}_h$ that intersect e.

(2) For the velocity: We introduce a variant of R_h denoted by $\mathcal{F}_h$ that is stable over $L^p(\Omega)^d$:

$$\|\mathcal{F}_h \mathbf{u}\|_{L^p(\Omega)^d} \leq C_p \|\mathbf{u}\|_{L^p(\Omega)^d}, \quad \text{for all } p \geq 1. \tag{23}$$

(see Appendix in [23])

(3) For the pressure: Let r_h be a Clément-type interpolation operator [15]. We have the following error estimate: for all κ in $\mathcal{T}_h$, for all e in $\partial\kappa$ and for all $q \in W^{1,3/2}(\Omega)$,

$$\|q - r_h q\|_{L^{3/2}(\kappa)} \leq c_\kappa h_\kappa |q|_{W^{1,3/2}(w_\kappa)} \tag{24}$$

and

$$\|q - r_h q\|_{L^{3/2}(e)} \leq c_e h_e^{1/3} |q|_{W^{1,3/2}(w_e)}, \tag{25}$$

where $c_e > 0$ and $c_\kappa > 0$ are constants independent of h, and ω_κ is the union of elements of $\mathcal{T}_h$ that intersect κ, including κ itself.

We recall the following theorem of *a priori* error estimates betwen the exact solution $(\mathbf{u}, p, C)$ of Problem (V_a) and discrete solution $(\mathbf{u}_h, p_h, C_h)$ of Problem (V_{ah}) [36]:

Theorem 3.1. *Under Assumption 1.1, let $(\mathbf{u}_h, p_h, C_h)$ be a solution of problem (V_{ah}), and $(\mathbf{u}, p, C)$ be a solution of problem (V_a). If $(\mathbf{u}, p, C)$ are such that $C \in H^2(\Omega)$, $\mathbf{u} \in W^{1,3}(\Omega)^d$ and $p \in H^2(\Omega)$, and satisfies the following condition:*

$$S_6^0 |C|_{W^{1,3}(\Omega)} + \| C \|_{L^\infty(\Omega)} \leq \frac{\alpha\mu K_m}{2\sqrt{2}\rho c_{\mathbf{f}_1} S_2^0}, \tag{26}$$

then, we have the following a priori error estimates:

$$|C - C_h|_{H^1(\Omega)} + \| \mathbf{u} - \mathbf{u}_h \|_{L^2(\Omega)^d} + \| \nabla(p - p_h) \|_{L^{\frac{3}{2}}(\Omega)^d} \leq c_1 h \tag{27}$$

and

$$\| \mathbf{u} - \mathbf{u}_h \|_{L^3(\Omega)^d} \leq c_2 h^{2/3}, \tag{28}$$

where c_1 and c_2 are strictly positive constants independent of h.

The following proposition gives a bound for the discrete velocity in $L^6(\Omega)^d$ which will be used in Section 4.

Proposition 3.2. *Under the assumptions of Theorem 3.1, we have the following bound:*

$$\|\mathbf{u}_h\|_{L^6(\Omega)^d} \leq \hat{c}(\mathbf{u}, p, C) \tag{29}$$

where $\hat{c}(\mathbf{u}, p, C)$ is a positive constant independent of h.

Proof. As $\mathbf{u} \in W^{1,3}(\Omega)^d \subset L^6(\Omega)^d$, and using a triangle inequality, we start from the following bound

$$\|\mathbf{u}_h\|_{L^6(\Omega)^d} \leq \|\mathbf{u}_h - \mathcal{F}_h u\|_{L^6(\Omega)^d} + \|\mathcal{F}_h u\|_{L^6(\Omega)^d} .$$

Using the fact that the operator $\mathcal{F}_h$ is stable over $L^6(\Omega)^d$ (relation (23) for $p = 6$), and that the mesh is uniformly regular, we get the bound

$$\begin{aligned} \|\mathbf{u}_h\|_{L^6(\Omega)^d} &\leq ch^{-d/3} \|\mathbf{u}_h - \mathcal{F}_h u\|_{L^2(\Omega)^d} + c\,\|\mathbf{u}\|_{L^6(\Omega)^d} \\ &\leq ch^{-d/3}(\|\mathbf{u}_h - \mathbf{u}\|_{L^2(\Omega)^d} + \|\mathbf{u} - \mathcal{F}_h u\|_{L^2(\Omega)^d}) + c\,\|\mathbf{u}\|_{L^6(\Omega)^d} . \end{aligned} \tag{30}$$

Finally, using the *a priori* error estimates, the properties of the operator $\mathcal{F}_h$, we get the desired result.

□

3.2. Successive approximations. As the problem is nonlinear, we introduce a straightforward successive approximation algorithm (see [36]) which converges to the discrete solution $(\mathbf{u}_h, p_h, C_h)$ of Problem (V_{ah}) under suitable conditions. The algorithm proceeds as follows: let $\mathbf{u}_0^h \in X_h$ and $C_h^0 \in Y_0$ the initial guesses. Having $(\mathbf{u}_h^i, C_h^i) \in X_h \times Y_h$ at each iteration i, we compute $(\mathbf{u}_h^{i+1}, p_h^{i+1}, C_h^{i+1}) \in X_h \times M_h \times Y_h$, such that

$$(V_{ahi}) \begin{cases} \forall \mathbf{v}_h \in X_h,\ \gamma \int_\Omega (\mathbf{u}_h^{i+1} - \mathbf{u}_h^i) \cdot \mathbf{v}_h d\mathbf{x} + \frac{\mu}{\rho} \int_\Omega (K^{-1}\mathbf{u}_h^{i+1}) \cdot \mathbf{v}_h \, d\mathbf{x} \\ \qquad + \dfrac{\beta}{\rho} \displaystyle\int_\Omega |\mathbf{u}_h^i| \mathbf{u}_h^{i+1} \cdot \mathbf{v}_h \, d\mathbf{x} + \int_\Omega \nabla p_h^{i+1} \cdot \mathbf{v}_h \, d\mathbf{x} = \int_\Omega \mathbf{f}(C_h^i) \cdot \mathbf{v}_h \, d\mathbf{x}, \\ \forall q_h \in M_h,\ \int_\Omega \nabla q_h \cdot \mathbf{u}_h^{i+1} \, d\mathbf{x} = 0, \\ \forall S_h \in Y_h,\ \alpha \displaystyle\int_\Omega \nabla C_h^{i+1} \cdot \nabla S_h \, d\mathbf{x} + \int_\Omega (\mathbf{u}_h^{i+1} \cdot \nabla C_h^{i+1}) S_h \, d\mathbf{x} \\ \qquad + \dfrac{1}{2} \displaystyle\int_\Omega \operatorname{div}(\mathbf{u}_h^{i+1})\, C_h^{i+1} S_h d\mathbf{x} + r_0 \int_\Omega C_h^{i+1} S_h \, d\mathbf{x} = \int_\Omega g S_h \, d\mathbf{x}, \end{cases}$$

where γ is a real strictly positive parameter. Later on, the parameter γ will be chosen to ensure the convergence of algorithm (V_{ahi}). At each iteration i, having $\mathbf{u}_h^i$ and C_h^i, the first two lines of (V_{ahi}) computes $(\mathbf{u}_h^{i+1}, p_h^{i+1})$. Next, we substitute $\mathbf{u}_h^{i+1}$ by its value in the third equation of (V_{ahi}) to compute C_h^{i+1}.

The additional term $\gamma \int_\Omega (\mathbf{u}_h^{i+1} - \mathbf{u}_h^i) \cdot \mathbf{v}_h d\mathbf{x}$ was added to ensure the convergence of the algorithm by calibrating the parameter γ. In fact, without this additional term, the convergence becomes more complex and requires additional assumptions on the exact solution.

For the existence and uniqueness of the solution of problem (V_{ahi}), we recall the following theorems (see [36]) with few modifications that give the parameter γ explicitly. The main ideas in the proof are exactly the same but for the reader convenience, we detailed some steps.

Theorem 3.3. *In addition to assumption 1.1, we suppose that* $\mathbf{f}_0 \in L^2(\Omega)^d$. *For each* $(\mathbf{u}_h^i, C_h^i) \in X_h \times Y_h$, *problem* (V_{ahi}) *admits a unique solution* $(\mathbf{u}_h^{i+1}, p_h^{i+1}, C_h^{i+1}) \in X_h \times M_h \times Y_h$. *Moreover, we have the following bound*

$$|C_h^{i+1}|_{1,\Omega} \le \frac{S_2^0}{\alpha} \|g\|_{L^2(\Omega)}. \tag{31}$$

Furthermore, if the initial value $\mathbf{u}_h^0$ *satisfies the condition*

$$\left\|\mathbf{u}_h^0\right\|_{L^2(\Omega)^d} \le L_1(\mathbf{f}, g), \tag{32}$$

where

$$L_1(\mathbf{f}, g) = \frac{\rho}{\mu K_m}(\|\mathbf{f}_0\|_{L^2(\Omega)^d} + c_{\mathbf{f}_1}\frac{(S_2^0)^2}{\alpha}\|g\|_{L^2(\Omega)}),$$

and if $\gamma \ge \gamma_*$ *with*

$$\begin{aligned}\gamma_* = {}& \frac{32\beta}{27\rho}c_I^3 h^{-d/2}\left(\frac{\rho}{\mu K_m} + \frac{\rho K_M}{\mu K_m^2}\right)\left(\|\mathbf{f}_0\|_{L^2(\Omega)^d} + c_{\mathbf{f}_1}\frac{(S_2^0)^2}{\alpha}\|g\|_{L^2(\Omega)}\right) \\ & + \frac{32\beta^2}{27\rho\mu^3 K_m^3}c_I^6 h^{-d}\left(\|\mathbf{f}_0\|_{L^2(\Omega)^d} + c_{\mathbf{f}_1}\frac{(S_2^0)^2}{\alpha}\|g\|_{L^2(\Omega)}\right)^2,\end{aligned} \tag{33}$$

then, the following inequalities hold

$$\left\|\mathbf{u}_h^{i+1}\right\|_{L^2(\Omega)^d} \le L_1(\mathbf{f}, g), \tag{34}$$

and

$$\left\|\mathbf{u}_h^{i+1}\right\|^3_{L^3(\Omega)^d} \le (\frac{\mu K_m}{\beta} + \frac{\gamma\rho}{\beta})L_1^2(\mathbf{f}, g). \tag{35}$$

Proof. To prove the existence and uniqueness of the solution of Problem (V_{ahi}) which is a square finite dimension linear system, it suffices to show the uniqueness which is readily checked for each $(\mathbf{u}_h^i, C_h^i) \in X_h \times Y_h$. In fact, let $(\mathbf{u}_{h,1}^{i+1}, p_{h,1}^{i+1}, C_{h,1}^{i+1})$ and $(\mathbf{u}_{h,2}^{i+1}, p_{h,2}^{i+1}, C_{h,2}^{i+1})$ be two solutions of problem (V_{ahi}). Denote $\mathbf{w}_h = \mathbf{u}_{h,1}^{i+1} - \mathbf{u}_{h,2}^{i+1}$ and $\xi_h = p_{h,1}^{i+1} - p_{h,2}^{i+1}$. We deduce from the problem (V_{ahi}) that $(\mathbf{w}_h, \xi_h)$ is the solution of the following problem

$$\begin{cases}\forall v_h \in X_h, \quad \gamma\displaystyle\int_\Omega \mathbf{w}_h\cdot\mathbf{v}_h\,d\mathbf{x} + \frac{\mu}{\rho}\int_\Omega K^{-1}\mathbf{w}_h\cdot\mathbf{v}_h\,d\mathbf{x} \\ \qquad\qquad + \frac{\beta}{\rho}\int_\Omega |\mathbf{u}_h^i|\mathbf{w}_h\cdot\mathbf{v}_h\,d\mathbf{x} + \int_\Omega \nabla\xi_h\cdot\mathbf{v}_h\,d\mathbf{x} = 0, \\ \forall q_h \in M_h, \quad \displaystyle\int_\Omega \nabla q_h\cdot\mathbf{w}_h\,d\mathbf{x} = 0.\end{cases}$$

Taking $(\mathbf{v}_h, q_h) = (\mathbf{w}_h, \xi_h)$ and remarking that $\int_\Omega |\mathbf{u}_h^i||\mathbf{w}_h|^2\,d\mathbf{x}$ is non negative, we obtain by using the properties of K^{-1}, the following bound

$$\left(\gamma + \frac{\mu K_m}{\rho}\right)\|\mathbf{w}_h\|^2_{L^2(\Omega)^d} \le 0.$$

Thus, we deduce that $\mathbf{w}_h = 0$ ($\mathbf{u}_{h,1}^{i+1} = \mathbf{u}_{h,2}^{i+1}$). The discrete inf-sup condition (20) implies that $\xi_h = 0$ ($p_{h,1}^{i+1} = p_{h,2}^{i+1}$). This gives the uniqueness of the velocity and the pressure for each iteration i.

Let us now prove the uniqueness of the concentration. We denote by $C_h^{i+1} =$

$C_{h,1}^{i+1} - C_{h,2}^{i+1}$. Then, the third equation of problem (V_{ahi}) gives: Find $C_h^{i+1} \in Y_h$ such that for all $S_h \in Y_h$

$$\alpha \int_\Omega \nabla C_h^{i+1} \cdot \nabla S_h \, d\mathbf{x} + \int_\Omega (\mathbf{u}_h^{i+1} \cdot \nabla C_h^{i+1}) S_h \, d\mathbf{x} + \frac{1}{2} \int_\Omega \mathrm{div}(\mathbf{u}_h^{i+1}) \, C_h^{i+1} S_h d\mathbf{x} + r_0 \int_\Omega C_h^{i+1} S_h \, d\mathbf{x} = 0, \tag{36}$$

where $(\mathbf{u}_h^{i+1}, p_h^{i+1})$ is the unique solution of the first two equations of problem (V_{ahi}). By taking $S_h = C_h^{i+1}$ and using the antisymmetric property we get the uniqueness of the concentration.

The bound (31) can be deduced immediately by taking $S_h = C_h^{i+1}$ in the third equation of problem (V_{ahi}), and by using the Cauchy-Schwartz inequality.
To prove the bound (34), we need first to estimate the error $\left\| \mathbf{u}_h^{i+1} - \mathbf{u}_h^i \right\|_{L^2(\Omega)^d}$ in terms of the previous value $\mathbf{u}_h^i$. Taking the first equation of problem (V_{ahi}) with $\mathbf{v}_h = \mathbf{u}_h^{i+1} - \mathbf{u}_h^i \in V_h$ yields

$$\gamma \left\| \mathbf{u}_h^{i+1} - \mathbf{u}_h^i \right\|^2_{L^2(\Omega)^d} + \frac{\mu}{\rho} \int_\Omega K^{-1} \mathbf{u}_h^{i+1} \cdot (\mathbf{u}_h^{i+1} - \mathbf{u}_h^i) d\mathbf{x} + \frac{\beta}{\rho} \int_\Omega |\mathbf{u}_h^i| \mathbf{u}_h^{i+1} \cdot (\mathbf{u}_h^{i+1} - \mathbf{u}_h^i) d\mathbf{x} = \int_\Omega \mathbf{f}(C_h^i) \cdot (\mathbf{u}_h^{i+1} - \mathbf{u}_h^i) d\mathbf{x}.$$

By inserting $\mathbf{u}_h^i$ in the second and third terms of the last equation, we get,

$$\begin{aligned} &\gamma \left\| \mathbf{u}_h^{i+1} - \mathbf{u}_h^i \right\|^2_{L^2(\Omega)^d} + \frac{\mu}{\rho} \int_\Omega K^{-1} (\mathbf{u}_h^{i+1} - \mathbf{u}_h^i) \cdot (\mathbf{u}_h^{i+1} - \mathbf{u}_h^i) \, d\mathbf{x} \\ &+ \frac{\beta}{\rho} \int_\Omega |\mathbf{u}_h^i| |\mathbf{u}_h^{i+1} - \mathbf{u}_h^i|^2 \, d\mathbf{x} \\ &= \int_\Omega \mathbf{f}(C_h^i) \cdot (\mathbf{u}_h^{i+1} - \mathbf{u}_h^i) \, d\mathbf{x} - \frac{\mu}{\rho} \int_\Omega K^{-1} \mathbf{u}_h^i \cdot (\mathbf{u}_h^{i+1} - \mathbf{u}_h^i) \, d\mathbf{x} \\ &- \frac{\beta}{\rho} \int_\Omega |\mathbf{u}_h^i| \mathbf{u}_h^i \cdot (\mathbf{u}_h^{i+1} - \mathbf{u}_h^i) \, d\mathbf{x}. \end{aligned} \tag{37}$$

Using the properties of K^{-1}, the Cauchy-Schwartz inequality and relation (16) give the following

$$\begin{aligned} &\gamma \left\| \mathbf{u}_h^{i+1} - \mathbf{u}_h^i \right\|^2_{L^2(\Omega)^d} + \frac{\mu K_m}{\rho} \left\| \mathbf{u}_h^{i+1} - \mathbf{u}_h^i \right\|^2_{L^2(\Omega)^d} \\ &\le \left\| \mathbf{f}(C_h^i) \right\|_{L^2(\Omega)^d} \left\| \mathbf{u}_h^{i+1} - \mathbf{u}_h^i \right\|_{L^2(\Omega)^d} + \frac{\mu K_M}{\rho} \left\| \mathbf{u}_h^{i+1} - \mathbf{u}_h^i \right\|_{L^2(\Omega)^d} \left\| \mathbf{u}_h^i \right\|_{L^2(\Omega)^d} \\ &+ \frac{\beta}{\rho} C_I^3 h^{-d/2} \left\| \mathbf{u}_h^i \right\|^2_{L^2(\Omega)^d} \left\| \mathbf{u}_h^{i+1} - \mathbf{u}_h^i \right\|_{L^2(\Omega)^d}. \end{aligned} \tag{38}$$

We simplify by $\left\| \mathbf{u}_h^{i+1} - \mathbf{u}_h^i \right\|_{L^2(\Omega)^d}$ to obtain:

$$\begin{aligned} &(\gamma + \frac{\mu K_m}{\rho}) \| \mathbf{u}_h^{i+1} - \mathbf{u}_h^i \|_{L^2(\Omega)^d} \\ &\le \| \mathbf{f}(C_h^i) \|_{L^2(\Omega)^d} + \frac{\mu K_M}{\rho} \| \mathbf{u}_h^i \|_{L^2(\Omega)^d} + \frac{\beta}{\rho} c_I^3 h^{-\frac{d}{2}} \| \mathbf{u}_h^i \|^2_{L^2(\Omega)^d}. \end{aligned}$$

Using the properties of $\mathbf{f}$ and the bound of the concentration (31), we get the following estimate:

$$\| \mathbf{u}_h^{i+1} - \mathbf{u}_h^i \|_{L^2(\Omega)^d} \le L_2(\mathbf{f}, g, \| \mathbf{u}_h^i \|_{L^2(\Omega)^d}), \tag{39}$$

where

$$L_2(\mathbf{f},g,\eta)=\frac{\rho}{\mu K_m}\Big(\|\mathbf{f}_0\|_{L^2(\Omega)^d}+c_{\mathbf{f}_1}\frac{(S_2^0)^2}{\alpha}\|g\|_{L^2(\Omega)}+\frac{\mu K_M}{\rho}\eta+\frac{\beta}{\rho}c_I^3h^{-\frac{d}{2}}\eta^2\Big),\quad \eta\in\mathbb{R}_+.$$

Then, we are now in position to show relation (34). We consider the first equation of problem (V_{ahi}) with $\mathbf{v}_h=\mathbf{u}_h^{i+1}$, and obtain

$$\begin{aligned}&\gamma\int_\Omega(\mathbf{u}_h^{i+1}-\mathbf{u}_h^i)\cdot\mathbf{u}_h^{i+1}\,d\mathbf{x}+\frac{\mu}{\rho}\int_\Omega K^{-1}\mathbf{u}_h^{i+1}\cdot\mathbf{u}_h^{i+1}\,d\mathbf{x}+\frac{\beta}{\rho}\left\|\mathbf{u}_h^{i+1}\right\|^3_{L^3(\Omega)^d}\\&\quad=\int_\Omega\mathbf{f}(C_h^i)\cdot\mathbf{u}_h^{i+1}\,d\mathbf{x}+\frac{\beta}{\rho}\int_\Omega(|\mathbf{u}_h^{i+1}|-|\mathbf{u}_h^i|)|\mathbf{u}_h^{i+1}|^2\,d\mathbf{x}.\end{aligned}\tag{40}$$

Using the properties of K^{-1}, the Cauchy-Schwarz inequality and the relations $ab\le\frac{1}{2\varepsilon}a^2+\frac{\varepsilon}{2}b^2$ and $a^2b\le\frac{1}{3}(\frac{1}{\delta^3}b^3+2\delta^{\frac{3}{2}}a^3)$ with $\varepsilon=\frac{\mu K_m}{\rho}$ and $\delta=(\frac{3\beta}{4\rho})^{2/3}$, we get

$$\begin{aligned}&\frac{\gamma}{2}\left\|\mathbf{u}_h^{i+1}\right\|^2_{L^2(\Omega)^d}-\frac{\gamma}{2}\left\|\mathbf{u}_h^{i}\right\|^2_{L^2(\Omega)^d}+\frac{\gamma}{2}\left\|\mathbf{u}_h^{i+1}-\mathbf{u}_h^i\right\|^2_{L^2(\Omega)^d}\\&\quad+\frac{\mu K_m}{2\rho}\left\|\mathbf{u}_h^{i+1}\right\|^2_{L^2(\Omega)^d}+\frac{\beta}{2\rho}\left\|\mathbf{u}_h^{i+1}\right\|^3_{L^3(\Omega)^d}\\&\quad\le\frac{\rho}{2\mu K_m}\left\|\mathbf{f}(C_h^i)\right\|^2_{L^2(\Omega)^d}+\frac{16\beta}{27\rho}c_I^3h^{-d/2}\left\|\mathbf{u}_h^{i+1}-\mathbf{u}_h^i\right\|^3_{L^2(\Omega)^d}.\end{aligned}\tag{41}$$

We denote by

$$c_1(\left\|\mathbf{u}_h^i\right\|_{L^2(\Omega)^d})=\frac{\gamma}{2}-\frac{16\beta}{27\rho}c_I^3h^{-d/2}L_2(\mathbf{f},g,\left\|\mathbf{u}_h^i\right\|_{L^2(\Omega)^d})$$

which is not necessarily positive at this level. Therefore, by using the bound (39), we obtain the following bound:

$$\begin{aligned}&\frac{\gamma}{2}\left\|\mathbf{u}_h^{i+1}\right\|^2_{L^2(\Omega)^d}-\frac{\gamma}{2}\left\|\mathbf{u}_h^{i}\right\|^2_{L^2(\Omega)^d}+c_1(\left\|\mathbf{u}_h^i\right\|_{L^2(\Omega)^d})\left\|\mathbf{u}_h^{i+1}-\mathbf{u}_h^i\right\|^2_{L^2(\Omega)^d}\\&\quad+\frac{\mu K_m}{2\rho}\left\|\mathbf{u}_h^{i+1}\right\|^2_{L^2(\Omega)^d}+\frac{\beta}{2\rho}\left\|\mathbf{u}_h^{i+1}\right\|^3_{L^3(\Omega)^d}\le\frac{\mu K_m}{2\rho}L_1^2(\mathbf{f},g).\end{aligned}\tag{42}$$

We now prove estimate (34) by induction on $i\ge1$ under some condition on γ that we will determine. Starting with relation (32), we suppose that we have

$$\left\|\mathbf{u}_h^i\right\|_{L^2(\Omega)^d}\le L_1(\mathbf{f},g).\tag{43}$$

We have two situations:

- $\left\|\mathbf{u}_h^{i+1}\right\|_{L^2(\Omega)^d}\le\left\|\mathbf{u}_h^i\right\|_{L^2(\Omega)^d}$, which immediately leads to
$$\left\|\mathbf{u}_h^{i+1}\right\|_{L^2(\Omega)^d}\le L_1(\mathbf{f},g).$$
- $\left\|\mathbf{u}_h^{i+1}\right\|_{L^2(\Omega)^d}\ge\left\|\mathbf{u}_h^i\right\|_{L^2(\Omega)^d}$. By using the induction condition (43) and the fact that the function L_2 is increasing with respect to η, we chose
$$\begin{aligned}\frac{\gamma}{2}&\ge\frac{16\beta}{27\rho}c_I^3h^{-d/2}L_2(\mathbf{f},g,L_1(\mathbf{f},g))\\&\ge\frac{16\beta}{27\rho}c_I^3h^{-d/2}L_2(\mathbf{f},g,\left\|\mathbf{u}_h^i\right\|_{L^2(\Omega)^d}),\end{aligned}\tag{44}$$
to get $c_1(\left\|\mathbf{u}_h^i\right\|_{L^2(\Omega)^d})\ge0$, and deduce from relation (42) that
$$\left\|\mathbf{u}_h^{i+1}\right\|_{L^2(\Omega)^d}\le L_1(\mathbf{f},g).$$

Then relation (34) holds. The bound (35) is a simple consequence of (42) and (34). Now we focus on the inequality (44). It is easy to show that $\forall \eta \in \mathbb{R}_+$,

$$L_2(\mathbf{f}, g, \eta) \leq \frac{\rho}{\mu K_m}(\|\mathbf{f}_0\|_{L^2(\Omega)^d} + \frac{c_{\mathbf{f}_1}(S_2^0)^2}{\alpha}\|g\|_{L^2(\Omega)}) + \frac{K_M}{K_m}\eta + \frac{\beta}{\rho}c_I^3 h^{-\frac{d}{2}}\frac{\rho}{\mu K_m}\eta^2, \tag{45}$$

and then to get by using the definition of L_1:

$$\begin{aligned} L_2(\mathbf{f}, g, L_1(\mathbf{f}, g)) \leq & (\frac{\rho}{\mu K_m} + \frac{\rho K_M}{\mu K_m^2})\left(\|\mathbf{f}_0\|_{L^2(\Omega)^d} + c_{\mathbf{f}_1}\frac{(S_2^0)^2}{\alpha}\|g\|_{L^2(\Omega)}\right) \\ & + \frac{\beta\rho^2}{\mu^3 K_m^3}c_I^3 h^{-d/2}\left(\|\mathbf{f}_0\|_{L^2(\Omega)^d} + c_{\mathbf{f}_1}\frac{(S_2^0)^2}{\alpha}\|g\|_{L^2(\Omega)}\right)^2. \end{aligned} \tag{46}$$

Relation (44) and the last inequality allow us to obtain

$$\frac{\gamma}{2} - \frac{16\beta}{27\rho}c_I^3 h^{-d/2} L_2(\mathbf{f}, g, L_1(\mathbf{f}, g)) \geq \phi(\gamma)$$

with

$$\begin{aligned} \phi(\gamma) = & \frac{\gamma}{2} - \frac{16\beta}{27\rho}c_I^3 h^{-d/2}\left(\frac{\rho}{\mu K_m} + \frac{\rho K_M}{\mu K_m^2}\right)\left(\|\mathbf{f}_0\|_{L^2(\Omega)^d} + c_{\mathbf{f}_1}\frac{(S_2^0)^2}{\alpha}\|g\|_{L^2(\Omega)}\right) \\ & - \frac{16\beta^2}{27\rho\mu^3 K_m^3}c_I^6 h^{-d}\left(\|\mathbf{f}_0\|_{L^2(\Omega)^d} + c_{\mathbf{f}_1}\frac{(S_2^0)^2}{\alpha}\|g\|_{L^2(\Omega)}\right)^2. \end{aligned} \tag{47}$$

We remark that $\phi(\gamma)$ is a polynomial of first degree with respect to γ with only root $\gamma_* > 0$. Finally, we get $\phi(\gamma) \geq 0$ for all $\gamma \geq \gamma_*$. □

We mention that the bounds of the iterative velocity ((34) and (35)) are obtained under the condition $\gamma \geq \gamma_*$. It is important to note that γ_* is not easy to compute and depends on the mesh step h.

The next theorem shows the convergence of the solution $(\mathbf{u}_h^i, p_h^i, C_h^i)$ of problem (V_{ahi}) to the discrete solution $(\mathbf{u}_h, p_h, C_h)$ of problem (V_{ah}).

Theorem 3.4. *Under the assumption of Theorem 3.3, we assume that the concentration solution of the problem (V_a) satisfies*

$$S_6^0|C|_{W^{1,3}(\Omega)} + \|C\|_{L^\infty(\Omega)} \leq \frac{\mu K_m \alpha}{2\rho c_{\mathbf{f}_1} S_2^0}. \tag{48}$$

Moreover, if γ satisfies the condition

$$\gamma > \max\{\gamma_*, \gamma_{**}\}, \tag{49}$$

where

$$\gamma_{**} = \frac{2\rho\beta^2 c_I^6 h^{-d}}{\mu^3 K_m^3}\left(\|\mathbf{f}_0\|_{L^2(\Omega)^d} + c_{\mathbf{f}_1}\frac{(S_2^0)^2}{\alpha}\|g\|_{L^2(\Omega)}\right)^2$$

and if

$$h \leq \left(\frac{1}{2c_I c_1}(|C|_{W^{1,3}(\Omega)} + \frac{\|C\|_{L^\infty(\Omega)}}{S_6^0})\right)^{6/(6-d)}, \tag{50}$$

where c_1 is the constant in (27), then the solution $(\mathbf{u}_h^i, p_h^i, C_h^i)$ of problem (V_{ahi}) converges in $L^2(\Omega)^d \times L^2(\Omega) \times H^1(\Omega)$ to the solution of problem (V_{ah}).

Proof. We start by substracting the third equation of problem (V_{ahi}) from the one of problem (V_{ah}) to get

$$
\begin{aligned}
&\alpha \int_\Omega \nabla(C_h - C_h^{i+1}) \cdot \nabla S_h \, d\mathbf{x} + \int_\Omega \mathbf{u}_h \cdot \nabla C_h S_h \, d\mathbf{x} \\
&- \int_\Omega \mathbf{u}_h^{i+1} \cdot \nabla C_h^{i+1} S_h \, d\mathbf{x} + r_0 \int_\Omega (C_h - C_h^{i+1}) S_h \, d\mathbf{x} \\
&= \frac{1}{2} \int_\Omega \operatorname{div} \mathbf{u}_h^{i+1} C_h^{i+1} S_h \, d\mathbf{x} - \frac{1}{2} \int_\Omega \operatorname{div} \mathbf{u}_h C_h S_h \, d\mathbf{x}.
\end{aligned} \tag{51}
$$

Inserting ∇C_h in the last term of the left-hand side and C_h in the first term of the right-hand side of the previous relation lead to

$$
\begin{aligned}
&\alpha \int_\Omega \nabla(C_h - C_h^{i+1}) \cdot \nabla S_h \, d\mathbf{x} + r_0 \int_\Omega (C_h - C_h^{i+1}) S_h \, d\mathbf{x} \\
&- \int_\Omega \mathbf{u}_h^{i+1} \cdot \nabla(C_h^{i+1} - C_h) S_h \, d\mathbf{x} \\
&= \frac{1}{2} \int_\Omega \operatorname{div} \mathbf{u}_h^{i+1} (C_h^{i+1} - C_h) S_h \, d\mathbf{x} + \int_\Omega (\mathbf{u}_h^{i+1} - \mathbf{u}_h) \cdot \nabla C_h S_h \, d\mathbf{x} \\
&+ \frac{1}{2} \int_\Omega \operatorname{div}(\mathbf{u}_h^{i+1} - \mathbf{u}_h) C_h S_h \, d\mathbf{x}.
\end{aligned} \tag{52}
$$

Finally, by inserting ∇C in the second term of right-hand side and using the Green's formula and the antisymmetric property, we get

$$
\begin{aligned}
&\alpha \int_\Omega \nabla(C_h - C_h^{i+1}) \cdot \nabla S_h \, d\mathbf{x} + r_0 \int_\Omega (C_h - C_h^{i+1}) S_h \, d\mathbf{x} \\
&= \frac{1}{2} \int_\Omega (\mathbf{u}_h^{i+1} - \mathbf{u}_h) \cdot \nabla(C_h - C) S_h \, d\mathbf{x} + \frac{1}{2} \int_\Omega (\mathbf{u}_h^{i+1} - \mathbf{u}_h) \cdot \nabla C S_h \, d\mathbf{x} \\
&- \frac{1}{2} \int_\Omega (\mathbf{u}_h^{i+1} - \mathbf{u}_h) \cdot \nabla S_h (C_h - C) \, d\mathbf{x} - \frac{1}{2} \int_\Omega (\mathbf{u}_h^{i+1} - \mathbf{u}_h) \cdot \nabla S_h C \, d\mathbf{x}.
\end{aligned} \tag{53}
$$

By taking $S_h = C_h - C_h^{i+1}$, we obtain

$$
\begin{aligned}
\alpha |C_h - C_h^{i+1}|_{1,\Omega} \le\ & S_6^0 \left\| \mathbf{u}_h^{i+1} - \mathbf{u}_h \right\|_{L^3(\Omega)^d} |C_h - C|_{1,\Omega} \\
&+ \frac{S_6^0}{2} \left\| \mathbf{u}_h^{i+1} - \mathbf{u}_h \right\|_{L^2(\Omega)^d} |C|_{W^{1,3}(\Omega)} \\
&+ \frac{1}{2} \|C\|_{L^\infty(\Omega)} \left\| \mathbf{u}_h^{i+1} - \mathbf{u}_h \right\|_{L^2(\Omega)^d}.
\end{aligned} \tag{54}
$$

Finally, we get by using relation (16):

$$
\begin{aligned}
|C_h - C_h^{i+1}|_{1,\Omega} \le & \frac{S_6^0}{2\alpha} \left[2 c_I h^{-d/6} |C - C_h|_{1,\Omega} + |C|_{W^{1,3}(\Omega)} + \frac{\|C\|_{L^\infty(\Omega)}}{S_6^0} \right] \\
& \cdot \left\| \mathbf{u}_h^{i+1} - \mathbf{u}_h \right\|_{L^2(\Omega)^d}.
\end{aligned} \tag{55}
$$

Furthermore, by taking the difference between the first equations of problems (V_{ah}) and (V_{ahi}) with $\mathbf{v}_h = \mathbf{u}_h^{i+1} - \mathbf{u}_h \in V_h$, we get

$$\begin{aligned}
&\frac{\gamma}{2}\left\|\mathbf{u}_h^{i+1}-\mathbf{u}_h\right\|^2_{L^2(\Omega)^d} - \frac{\gamma}{2}\left\|\mathbf{u}_h^{i}-\mathbf{u}_h\right\|^2_{L^2(\Omega)^d} + \frac{\gamma}{2}\left\|\mathbf{u}_h^{i+1}-\mathbf{u}_h^i\right\|^2_{L^2(\Omega)^d}\\
&+\frac{\mu}{\rho}\int_\Omega K^{-1}|\mathbf{u}_h^{i+1}-\mathbf{u}_h|^2\,d\mathbf{x} + \frac{\beta}{\rho}\int_\Omega (|\mathbf{u}_h^i| - |\mathbf{u}_h^{i+1}|)\mathbf{u}_h^{i+1}\cdot(\mathbf{u}_h^{i+1}-\mathbf{u}_h)d\mathbf{x}\\
&+\frac{\beta}{\rho}\int_\Omega (|\mathbf{u}_h^{i+1}|\mathbf{u}_h^{i+1} - |\mathbf{u}_h|\mathbf{u}_h)\cdot(\mathbf{u}_h^{i+1}-\mathbf{u}_h)d\mathbf{x}\\
&=\int_\Omega (\mathbf{f}(C_h^i) - \mathbf{f}(C_h)).(\mathbf{u}_h^{i+1}-\mathbf{u}_h)\,d\mathbf{x}.
\end{aligned} \tag{56}$$

By using the relation (13) and an inverse inequality we obtain,

$$\begin{aligned}
&\frac{\gamma}{2}\left\|\mathbf{u}_h^{i+1}-\mathbf{u}_h\right\|^2_{L^2(\Omega)^d} - \frac{\gamma}{2}\left\|\mathbf{u}_h^{i}-\mathbf{u}_h\right\|^2_{L^2(\Omega)^d}\\
&+\frac{\gamma}{2}\left\|\mathbf{u}_h^{i+1}-\mathbf{u}_h^i\right\|^2_{L^2(\Omega)^d} + \frac{\mu K_m}{\rho}\left\|\mathbf{u}_h^{i+1}-\mathbf{u}_h\right\|^2_{L^2(\Omega)^d}\\
&\le \frac{\beta}{\rho}\left\|\mathbf{u}_h^{i+1}-\mathbf{u}_h^i\right\|_{L^3(\Omega)^d}\left\|\mathbf{u}_h^{i+1}\right\|_{L^3(\Omega)^d}\left\|\mathbf{u}_h^{i+1}-\mathbf{u}_h\right\|_{L^3(\Omega)^d}\\
&+ c_{\mathbf{f}_1}S_2^0|C_h^i - C_h|_{1,\Omega}\left\|\mathbf{u}_h^{i+1}-\mathbf{u}_h\right\|_{L^2(\Omega)^d}\\
&\le \frac{\beta}{\rho}c_I^3 h^{-d/2}L_1(\mathbf{f},g)\left\|\mathbf{u}_h^{i+1}-\mathbf{u}_h^i\right\|_{L^2(\Omega)^d}\left\|\mathbf{u}_h^{i+1}-\mathbf{u}_h\right\|_{L^2(\Omega)^d}\\
&+ c_{\mathbf{f}_1}S_2^0|C_h^i - C_h|_{1,\Omega}\left\|\mathbf{u}_h^{i+1}-\mathbf{u}_h\right\|_{L^2(\Omega)^d}.
\end{aligned} \tag{57}$$

We denote by $c_2 = \dfrac{\beta}{\rho}c_I^3 L_1(\mathbf{f},g)$ and we use the relation $ab \le \dfrac{1}{2\varepsilon}a^2 + \dfrac{\varepsilon}{2}b^2$ with $\varepsilon = \dfrac{\mu K_m}{2\rho}$, we get

$$\begin{aligned}
&\frac{\gamma}{2}\left\|\mathbf{u}_h^{i+1}-\mathbf{u}_h\right\|^2_{L^2(\Omega)^d} - \frac{\gamma}{2}\left\|\mathbf{u}_h^{i}-\mathbf{u}_h\right\|^2_{L^2(\Omega)^d}\\
&+\frac{\gamma}{2}\left\|\mathbf{u}_h^{i+1}-\mathbf{u}_h^i\right\|^2_{L^2(\Omega)^d} + \frac{\mu K_m}{2\rho}\left\|\mathbf{u}_h^{i+1}-\mathbf{u}_h\right\|^2_{L^2(\Omega)^d}\\
&\le \frac{\rho c_2^2}{\mu K_m}h^{-d}\left\|\mathbf{u}_h^{i+1}-\mathbf{u}_h^i\right\|^2_{L^2(\Omega)^d} + \frac{\rho(c_{\mathbf{f}_1}S_2^0)^2}{\mu K_m}|C_h^i - C_h|^2_{1,\Omega}.
\end{aligned} \tag{58}$$

We then choose

$$\frac{\gamma}{2} > \frac{\rho c_2^2}{\mu K_m}h^{-d}, \tag{59}$$

and denote by $c_3 = \dfrac{\gamma}{2} - \dfrac{\rho c_2^2}{\mu K_m}h^{-d} > 0$, to conclude that

$$\begin{aligned}
&\frac{\gamma}{2}\left\|\mathbf{u}_h^{i+1}-\mathbf{u}_h\right\|^2_{L^2(\Omega)^d} - \frac{\gamma}{2}\left\|\mathbf{u}_h^{i}-\mathbf{u}_h\right\|^2_{L^2(\Omega)^d}\\
&+ c_3\left\|\mathbf{u}_h^{i+1}-\mathbf{u}_h^i\right\|^2_{L^2(\Omega)^d} + \frac{\mu K_m}{2\rho}\left\|\mathbf{u}_h^{i+1}-\mathbf{u}_h\right\|^2_{L^2(\Omega)^d}\\
&\le \frac{\rho(c_{\mathbf{f}_1}S_2^0)^2}{\mu K_m}|C_h^i - C_h|^2_{1,\Omega}.
\end{aligned} \tag{60}$$

Combining (60) with (55) and using the *a priori* error estimate (27), we get

$$(61)\quad \begin{aligned} &\frac{\gamma}{2}\left\|\mathbf{u}_h^{i+1}-\mathbf{u}_h\right\|^2_{L^2(\Omega)^d}-\frac{\gamma}{2}\left\|\mathbf{u}_h^{i}-\mathbf{u}_h\right\|^2_{L^2(\Omega)^d}\\ &+c_3\left\|\mathbf{u}_h^{i+1}-\mathbf{u}_h^{i}\right\|^2_{L^2(\Omega)^d}+\frac{\mu K_m}{2\rho}\left\|\mathbf{u}_h^{i+1}-\mathbf{u}_h\right\|^2_{L^2(\Omega)^d}\\ &\le \frac{\rho}{\mu K_m}(\frac{c_{\mathbf{f}_1}S_2^0S_6^0}{2\alpha})^2\left[2c_Ic_1h^{(6-d)/6}+|C|_{W^{1,3}(\Omega)}+\frac{\|C\|_{L^\infty(\Omega)}}{S_6^0}\right]^2\\ &\cdot\left\|\mathbf{u}_h^{i}-\mathbf{u}_h\right\|^2_{L^2(\Omega)^d}. \end{aligned}$$

Thus, Assumptions (48) and (50) allow us to get

$$(62)\quad \begin{aligned} &(\frac{\gamma}{2}+\frac{\mu K_m}{4\rho})\big(\left\|\mathbf{u}_h^{i+1}-\mathbf{u}_h\right\|^2_{L^2(\Omega)^d}-\left\|\mathbf{u}_h^{i}-\mathbf{u}_h\right\|^2_{L^2(\Omega)^d}\big)\\ &\quad+c_3\left\|\mathbf{u}_h^{i+1}-\mathbf{u}_h^{i}\right\|^2_{L^2(\Omega)^d}+\frac{\mu K_m}{4\rho}\left\|\mathbf{u}_h^{i+1}-\mathbf{u}_h\right\|^2_{L^2(\Omega)^d}\le 0. \end{aligned}$$

Finally, (59) is clearly satisfied if $\gamma > \gamma_{**}$.
Thus, the last inequality gives (if $\left\|\mathbf{u}_h^{i}-\mathbf{u}_h\right\|_{L^2(\Omega)^d}\neq 0$)

$$||\mathbf{u}_h^{i+1}-\mathbf{u}_h||_{L^2(\Omega)^d} < ||\mathbf{u}_h^{i}-\mathbf{u}_h||_{L^2(\Omega)^d},$$

so we deduce the convergence of the sequence $(\mathbf{u}_h^{i+1}-\mathbf{u}_h)$ in $L^2(\Omega)^d$ and then the convergence of the sequence $\mathbf{u}_h^i$ in $L^2(\Omega)^d$.
Finally, by taking the limit of equation (62), we get that the sequence $\mathbf{u}_h^{i+1}$ converges to $\mathbf{u}_h$ in $L^2(\Omega)^d$. The convergence of the concentration can be deduced from relation (55) and concerning the pressure, we refer to Theorem 4.2 in [36]. □

Remark 3.5. *In order to show the convergence of the algorithm, the assumptions of Theorems 3.3 and 3.4 require the smallness of the exact concentration C (see relation*(48)*) and the condition* (49) *which requires that γ must be bigger than a constant that is difficult to compute and depending on the mesh step h. Furthermore, Relation* (50) *demands that h must be smaller than a constant depending on the exact concentration C where $(\mathbf{u}, p, C)$ is the solution of (P).*

4. A posteriori error estimation

The *a posteriori* analysis controls the overall discretization error of a problem by providing error indicators that are easy to compute. Once these error indicators are constructed, their efficiency can be proven by bounding each indicator by the local error.
As usual, for *a posteriori* error estimates, we introduce the following notations. We denote by

- Γ_h^i the set of edges (when $d = 2$) or faces (when $d = 3$) of κ that are not contained in $\partial\Omega$.
- Γ_h^b the set of edges (when $d = 2$) or faces (when $d = 3$) of κ which are contained in $\partial\Omega$.

For every element κ in $\mathcal{T}_h$, we denote by w_κ the union of elements K of $\mathcal{T}_h$ such that $\kappa \cap K \neq \phi$. Furthermore, for every edge (when $d = 2$) or face (when $d = 3$) e of the mesh $\mathcal{T}_h$, we denote by

- ω_e the union of elements of $\mathcal{T}_h$ adjacent to e.
- $[\cdot]_e$ the jump through $e \in \Gamma_h^i$.

In this and the next sections, the *a posteriori* error estimates are established for slightly smoother solutions.

4.1. Upper error bound. In order to establish upper bounds, we introduce, on every edge ($d=2$) or face ($d=3$) e of the mesh, the function

$$\phi^e_{h,1} = \begin{cases} \frac{1}{2}\,[\mathbf{u}_h^{i+1}\cdot\mathbf{n}]_e & \text{if } e\in\Gamma_h^i,\\ \mathbf{u}_h^{i+1}\cdot\mathbf{n} & \text{if } e\in\Gamma_h^b. \end{cases} \tag{63}$$

A standard calculation shows that the solutions of problems (V_a) and (V_{ahi}) satisfy for all $(\mathbf{v},q,S)\in X\times M\times Y$ and $(\mathbf{v}_h,q_h,S_h)\in X_h\times M_h\times Y_h$:
(64)

$$\begin{aligned}
&\alpha\int_\Omega \nabla(C-C_h^{i+1})\cdot\nabla S\,d\mathbf{x}+\int_\Omega(\mathbf{u}\cdot\nabla C)S\,d\mathbf{x}-\int_\Omega(\mathbf{u}_h^{i+1}\cdot\nabla C_h^{i+1})S\,d\mathbf{x}\\
&\quad+r_0\int_\Omega CS\,d\mathbf{x}-r_0\int_\Omega C_h^{i+1}S\,d\mathbf{x}-\frac{1}{2}\int_\Omega \operatorname{div}\mathbf{u}_h^{i+1}C_h^{i+1}S\,d\mathbf{x}\\
&\quad=\sum_{\kappa\in\mathcal{T}_h}\Big[\int_\kappa (g-g_h)(S-S_h)\,d\mathbf{x}-\frac{\alpha}{2}\sum_{e\in\partial\kappa\cap\Gamma_h^i}\int_e[\nabla C_h^{i+1}\cdot\mathbf{n}]_e(S-S_h)\,ds\\
&\quad+\int_\kappa(\alpha\triangle C_h^{i+1}-\mathbf{u}_h^{i+1}\cdot\nabla C_h^{i+1}-\frac{1}{2}\operatorname{div}\mathbf{u}_h^{i+1}C_h^{i+1}-r_0C_h^{i+1}+g_h)(S-S_h)d\mathbf{x}\Big],
\end{aligned}$$

(65)

$$\begin{aligned}
&\frac{\mu}{\rho}\int_\Omega K^{-1}(\mathbf{u}-\mathbf{u}_h^{i+1})\cdot\mathbf{v}\,d\mathbf{x}+\frac{\beta}{\rho}\int_\Omega(|\mathbf{u}|\mathbf{u}-|\mathbf{u}_h^i|\mathbf{u}_h^{i+1})\cdot\mathbf{v}\,d\mathbf{x}+\int_\Omega\nabla(p-p_h^{i+1})\cdot\mathbf{v}\,d\mathbf{x}\\
&=\sum_{\kappa\in\mathcal{T}_h}\Big[\int_\kappa\big(-\nabla p_h^{i+1}-\gamma(\mathbf{u}_h^{i+1}-\mathbf{u}_h^i)-\frac{\mu}{\rho}K^{-1}\mathbf{u}_h^{i+1}\\
&-\frac{\beta}{\rho}|\mathbf{u}_h^i|\mathbf{u}_h^{i+1}+\mathbf{f}_h(C_h^i)\big)\cdot(\mathbf{v}-\mathbf{v}_h)\,d\mathbf{x}\\
&+\gamma\int_\kappa(\mathbf{u}_h^{i+1}-\mathbf{u}_h^i)\cdot\mathbf{v}\,d\mathbf{x}+\int_\kappa\big(\mathbf{f}(.,C)-\mathbf{f}_h(C)\big)\cdot\mathbf{v}\,d\mathbf{x}+\int_\kappa\big(\mathbf{f}_h(C)-\mathbf{f}_h(C_h^i)\big)\cdot\mathbf{v}\,d\mathbf{x}\\
&+\int_\kappa\big(\mathbf{f}_h(C_h^i)-\mathbf{f}(.,C_h^i)\big)\cdot\mathbf{v}_h\,d\mathbf{x}\Big],
\end{aligned}$$

and

$$\int_\Omega\nabla q\cdot(\mathbf{u}-\mathbf{u}_h^{i+1})\,d\mathbf{x}=\sum_{\kappa\in\mathcal{T}_h}\Big[\int_\kappa(q-q_h)\operatorname{div}\mathbf{u}_h^{i+1}\,d\mathbf{x}-\sum_{e\in\partial\kappa}\int_e\phi^e_{h,1}(q-q_h)ds\Big], \tag{66}$$

where g_h is an approximation of g and $\mathbf{f}_h$ is an approximation of $\mathbf{f}$. The approximations g_h and $\mathbf{f}_h$ are constants on each element κ of $\mathcal{T}_h$ given by :

$$\forall C\in Y,\forall\kappa\in\mathcal{T}_h,\quad \mathbf{f}_h(C)|_\kappa=\frac{1}{|\kappa|}\int_\kappa\mathbf{f}(.,C)(\mathbf{x})\,d\mathbf{x}.$$

Since $\mathbf{f}_1$ is $c_{\mathbf{f}_1}$ Lipschitz, we clearly have the following property :

$$\|\mathbf{f}_h(C_1)-\mathbf{f}_h(C_2)\|_{L^2(\kappa)}\le c_{\mathbf{f}_1}\|C_1-C_2\|_{L^2(\kappa)}\quad\forall(C_1,C_2)\in Y\times Y. \tag{67}$$

From the error equations (64)-(66), we deduce the following error indicators for each $\kappa\in\mathcal{T}_h$:

$$\eta^{(L_1)}_{\kappa,i}=\left\|\mathbf{u}_h^{i+1}-\mathbf{u}_h^i\right\|_{L^2(\kappa)}, \tag{68}$$

(69)
$$\eta_{\kappa,i}^{(L_2)} = ||C_h^i - C_h^{i+1}||_{H^1(\kappa)},$$

(70)
$$\begin{aligned}\eta_{\kappa,i}^{(D_1)} =& h_\kappa \left\| \alpha \triangle C_h^{i+1} - \mathbf{u}_h^{i+1} \cdot \nabla C_h^{i+1} - \frac{1}{2} \operatorname{div} \mathbf{u}_h^{i+1} C_h^{i+1} - r_0 C_h^{i+1} + g_h \right\|_{L^2(\kappa)} \\ &+ \frac{1}{2} \sum_{e \in \partial\kappa \cap \Gamma_h^i} h_e^{\frac{1}{2}} \left\| \alpha [\nabla C_h^{i+1} \cdot \mathbf{n}]_e \right\|_{L^2(e)},\end{aligned}$$

(71)
$$\eta_{\kappa,i}^{(D_2)} = \left\| -\nabla p_h^{i+1} - \gamma(\mathbf{u}_h^{i+1} - \mathbf{u}_h^i) - \frac{\mu}{\rho} K^{-1} \mathbf{u}_h^{i+1} - \frac{\beta}{\rho} |\mathbf{u}_h^i| \mathbf{u}_h^{i+1} + \mathbf{f}_h(C_h^i) \right\|_{L^2(\kappa)},$$

and

(72)
$$\eta_{\kappa,i}^{(D_3)} = h_\kappa \left\| \operatorname{div} \mathbf{u}_h^{i+1} \right\|_{L^3(\kappa)} + \sum_{e \in \partial\kappa} h_e^{\frac{1}{3}} \left\| \phi_{h,1}^e \right\|_{L^3(e)}.$$

The above indicators are of two types:

(1) $\eta_{\kappa,i}^{(L_1)}$ and $\eta_{\kappa,i}^{(L_2)}$: indicators of linearization (or iteration).

(2) $\eta_{\kappa,i}^{(D_1)}$, $\eta_{\kappa,i}^{(D_2)}$ and $\eta_{\kappa,i}^{(D_3)}$: indicators of discretization.

The first type expresses the errors between the exact and numerical solutions of two consecutive iterations while the second type gives the error provided from the discretization method (here the finite element method). One of the most important applications of these indicators in the adaptive mesh method (as we will see in the last section of this paper).

In order to establish the upper bound, we need to first bound the numerical solution $\mathbf{u}_h^{i+1}$ in $L^6(\Omega)^d$ in terms of the exact solution which is the subject of the next lemma.

Lemma 4.1. *Let the mesh satisfy* (14)*, under the assumptions of Theorem 3.1, Theorem 3.3, Theorem 3.4, there exists an integer i_0 depending on h such that for all $i \geq i_0$, the numerical velocity $\mathbf{u}_h^{i+1}$ satisfies the following bound :*

(73)
$$\left\| \mathbf{u}_h^{i+1} \right\|_{L^6(\Omega)^d} \leq \hat{c}_1(\mathbf{u}, p, C)$$

where $\hat{c}_1$ is a constant depending on the exact solution $(\mathbf{u}, p, C)$ of problem (V_a).

Proof. Let $(\mathbf{u}, p, C)$ be the solution of problem (V_a), $(\mathbf{u}_h, p_h, C_h)$ be the solution of (V_{ah}) and $(\mathbf{u}_h^{i+1}, p_h^{i+1}, C_h^{i+1})$ the solution of (V_{ahi}).

By using (16) (for $p = 6$) and the bound (29), the term $\|\mathbf{u}_h^{i+1}\|_{L^6(\Omega)}$ can be bounded as following:

(74)
$$\begin{aligned}\left\| \mathbf{u}_h^{i+1} \right\|_{L^6(\Omega)^d} &\leq \left\| \mathbf{u}_h^{i+1} - \mathbf{u}_h \right\|_{L^6(\Omega)^d} + \left\| \mathbf{u}_h \right\|_{L^6(\Omega)^d} \\ &\leq c_I h^{-d/3} \left\| \mathbf{u}_h^{i+1} - \mathbf{u}_h \right\|_{L^2(\Omega)^d} + \hat{c}(\mathbf{u}, p, C).\end{aligned}$$

As $\mathbf{u}_h^{i+1}$ converges to $\mathbf{u}_h$ in $L^2(\Omega)^d$, there exists an integer i_0 depending on h such that for all $i \geq i_0$ we have

(75)
$$\|\mathbf{u}_h^{i+1} - \mathbf{u}_h\|_{L^2(\Omega)^d} \leq h^{d/3}.$$

Then inequality (74) and (75) give the desired result (73).

□

Our main goal is to get an upper bound of the error between the exact solution $(\mathbf{u}, p, C)$ of problem (V_a) and the numerical solution $(\mathbf{u}_h^{i+1}, p_h^{i+1}, C_h^{i+1})$ of (V_{ahi}) in $X \times M \times Y$. In the next theorem we will bound the error of the velocity in $L^2(\Omega)^d$ with the indicators. Unfortunately, we couldn't bound the error $\mathbf{u} - \mathbf{u}_h^{i+1}$ in $L^3(\Omega)^d$ by the indicators but we will bound a part $\mathbf{v}_r$ of this error since we have (as we will see later) the decomposition $\mathbf{u} - \mathbf{u}_h^{i+1} = \mathbf{z}_0 + \mathbf{v}_r$. Furthermore, we will bound the error $\|\mathbf{u} - \mathbf{u}_h^{i+1}\|_{L^3(\Omega)^d}$ but with the indicators to the power 2/3 (instead of the power 1). The bound of the part $\mathbf{v}_r$ of $\mathbf{u} - \mathbf{u}_h^{i+1}$ is crucial for the efficiency of the method in the sense that the indicator $\eta_{K,i}^{(D_3)}$ will be bounded locally by $\mathbf{v}_r$ in L^3 (that is the reason why we introduce the part $\mathbf{v}_r$ of the velocity error).

We begin by introducing in the next lemma the part $\mathbf{v}_r$ of $\mathbf{u} - \mathbf{u}_h^{i+1}$:

Lemma 4.2. *There exists a velocity $\mathbf{v}_r$ in $L^3(\Omega)^d$ that solves the following variational problem:*

(76)
$$\forall q \in M, \quad \int_\Omega \nabla q \cdot \mathbf{v}_r \, d\mathbf{x} = \sum_{\kappa \in \mathcal{T}_h} \Big(\int_\kappa (q - r_h q) \operatorname{div} \mathbf{u}_h^{i+1} \, d\mathbf{x} - \sum_{e \in \partial_\kappa} \int_e \phi_{h,1}^e (q - r_h q) \, ds \Big)$$

which satisfies the following bound:

$$\| \mathbf{v}_r \|_{L^3(\Omega)^d} \leq c_2' \Big(\sum_{\kappa \in \mathcal{T}_h} (\eta_{\kappa,i}^{(D_3)}) \Big). \tag{77}$$

Proof. Using the equation (66) with $q_h = r_h q$, considering the inf-sup condition (11), and the fact that the right hand side term is a continuous linear function of q, we deduce the existence a velocity $\mathbf{v}_r$ in X such that (76) is verified, and satisfying the following bound:

$$\begin{aligned} \| \mathbf{v}_r \|_{L^3(\Omega)^d} \leq & \sup_{q \in M} \frac{1}{\|\nabla q\|_{L^{3/2}(\Omega)^3}} \Big| \sum_{\kappa \in \mathcal{T}_h} \big[\| q - r_h q \|_{L^{3/2}(\kappa)} \| \operatorname{div} \mathbf{u}_h^{i+1} \|_{L^3(\kappa)} \\ & + \sum_{e \in \partial\kappa} \| \phi_{h,1}^e \|_{L^3(e)} \| q - r_h q \|_{L^{3/2}(e)} \big] \Big|. \end{aligned} \tag{78}$$

Thus, from the properties of the operator r_h, the regularity of $\mathcal{T}_h$, and the following Hölder inequality, $(p = 3/2, q = 3)$

$$\sum_{k=1}^n a_k b_k \leq \big(\sum_{k=1}^n a_k^p \big)^{1/p} \big(\sum_{k=1}^n b_k^q \big)^{1/q},$$

we get after cubing the last equation:

$$\| \mathbf{v}_r \|_{L^3(\Omega)^d}^3 \leq c_2 \sum_{\kappa \in \mathcal{T}_h} \big(\eta_{\kappa,i}^{(D_3)} \big)^3, \tag{79}$$

with $c_2 > 0$ is a constant independent of h. Finally, we obtain the wanted result by taking the cubic root of the previous inequality. □

The next theorem states the upper bound of the error between the exact solution $(\mathbf{u}, p, C)$ of Problem (V_a) and the iterative solution of Problem (V_{ahi}):

Theorem 4.3. *Under the assumptions of Lemma 4.1, we suppose in addition that the exact solution $(\mathbf{u}, C)$ of Problem (V_a) satisfies: $\mathbf{u} \in L^\infty(\Omega)^d$ and*

$$S_6^0 |C|_{W^{1,3}(\Omega)} + \| C \|_{L^\infty(\Omega)} \leq \frac{\alpha}{c_{\mathbf{f}_1} S_2^0} \sqrt{\frac{\mu K_m}{\rho}}. \tag{80}$$

Then, there exists an integer i_0 depending on h such that $\forall i \geq i_0$, the solutions $(\mathbf{u}, p, C)$ and $(\mathbf{u}_h^{i+1}, p_h^{i+1}, C_h^{i+1})$ of problems (V_a) and (V_{ahi}) satisfy the following upper bound of error by the posteriori estimator:

$$
\begin{aligned}
&\| \mathbf{u} - \mathbf{u}_h^{i+1} \|_{L^2(\Omega)^d} + \left\| C - C_h^{i+1} \right\|_{H^1(\Omega)} + \| \mathbf{v}_r \|_{L^3(\Omega)^d} \\
&\leq \tilde{c}_3 \Big(\sum_{\kappa \in \mathcal{T}_h} \big(\eta_{\kappa,i}^{(D_1)} + \eta_{\kappa,i}^{(D_2)} + \eta_{\kappa,i}^{(D_3)} + \eta_{\kappa,i}^{(L_1)} \\
&+ \eta_{\kappa,i}^{(L_2)} + h_k \| g - g_h \|_{L^2(\kappa)} + \| \mathbf{f}(., C) - \mathbf{f}_h(C) \|_{L^2(\kappa)} \big) \Big)
\end{aligned}
\tag{81}
$$

where $\tilde{c}_3$ is a positive constant independent of h.

Proof. Let us start with the concentration equation (64) tested with $S = C - C_h^{i+1}$ and $S_h = R_h(S)$. It can be written as:
(82)

$$
\begin{aligned}
&\alpha |C - C_h^{i+1}|^2_{H^1(\Omega)} + r_0 \left\| C - C_h^{i+1} \right\|^2_{L^2(\Omega)} \\
&= - \int_\Omega (\mathbf{u} \cdot \nabla C) S \, d\mathbf{x} + \int_\Omega (\mathbf{u}_h^{i+1} \cdot \nabla C_h^{i+1}) S \, d\mathbf{x} + \frac{1}{2} \int_\Omega \operatorname{div} \mathbf{u}_h^{i+1} C_h^{i+1} S \, d\mathbf{x} \\
&+ \sum_{\kappa \in \mathcal{T}_h} \Big[\int_\kappa (g - g_h)(S - S_h) \, d\mathbf{x} - \frac{\alpha}{2} \sum_{e \in \partial\kappa \cap \Gamma_h^i} \int_e [\nabla C_h^{i+1} \cdot \mathbf{n}]_e (S - S_h) \, ds \\
&+ \int_\kappa (\alpha \triangle C_h^{i+1} - \mathbf{u}_h^{i+1} \cdot \nabla C_h^{i+1} - \frac{1}{2} \operatorname{div} \mathbf{u}_h^{i+1} C_h^{i+1} - r_0 C_h^{i+1} + g_h)(S - S_h) d\mathbf{x} \Big].
\end{aligned}
$$

By insterting $\mathbf{u}_h^{i+1}$ in the first term in the right-hand side of equation (82) and recalling that
$S = C - C_h^{i+1}$, the first three terms of the right-hand side in the previous equation can be written as :
(83)

$$
\begin{aligned}
&- \int_\Omega (\mathbf{u} \cdot \nabla C) S \, d\mathbf{x} + \int_\Omega (\mathbf{u}_h^{i+1} \cdot \nabla C_h^{i+1}) S \, d\mathbf{x} + \frac{1}{2} \int_\Omega \operatorname{div} \mathbf{u}_h^{i+1} C_h^{i+1} S \, d\mathbf{x} \\
&= - \int_\Omega ((\mathbf{u} - \mathbf{u}_h^{i+1}) \cdot \nabla C)(C - C_h^{i+1}) \, d\mathbf{x} \\
&- \int_\Omega (\mathbf{u}_h^{i+1} \cdot \nabla (C - C_h^{i+1})(C - C_h^{i+1}) \, d\mathbf{x} + \frac{1}{2} \int_\Omega \operatorname{div} \mathbf{u}_h^{i+1} C_h^{i+1} (C - C_h^{i+1}) \, d\mathbf{x}.
\end{aligned}
$$

By applying Green's formula and using the fact that the fluid is incompressible, the last two terms of (83) can be written as:

$$
\begin{aligned}
&- \int_\Omega (\mathbf{u}_h^{i+1} \cdot \nabla (C - C_h^{i+1})(C - C_h^{i+1}) \, d\mathbf{x} + \frac{1}{2} \int_\Omega \operatorname{div} \mathbf{u}_h^{i+1} C_h^{i+1} (C - C_h^{i+1}) \, d\mathbf{x} \\
&= \frac{1}{2} \int_\Omega \operatorname{div} \mathbf{u}_h^{i+1} C (C - C_h^{i+1}) \, d\mathbf{x} \\
&= -\frac{1}{2} \int_\Omega \operatorname{div} (\mathbf{u} - \mathbf{u}_h^{i+1}) C (C - C_h^{i+1}) \, d\mathbf{x} \\
&= \frac{1}{2} \int_\Omega (\mathbf{u} - \mathbf{u}_h^{i+1}) \cdot \big(\nabla C (C - C_h^{i+1}) + C \nabla (C - C_h^{i+1}) \big) \, d\mathbf{x}.
\end{aligned}
\tag{84}
$$

Thus, the right-hand side of Equation (83) can be written as

$$
\begin{aligned}
& -\int_\Omega ((\mathbf{u}-\mathbf{u}_h^{i+1})\cdot\nabla C)(C-C_h^{i+1})\,d\mathbf{x} \\
& -\int_\Omega (\mathbf{u}_h^{i+1}\cdot\nabla(C-C_h^{i+1})(C-C_h^{i+1})\,d\mathbf{x} \\
& +\frac{1}{2}\int_\Omega \operatorname{div}\mathbf{u}_h^{i+1}C_h^{i+1}(C-C_h^{i+1})\,d\mathbf{x} \\
& = -\frac{1}{2}\int_\Omega (\mathbf{u}-\mathbf{u}_h^{i+1})\cdot\big(\nabla C(C-C_h^{i+1})-C\nabla(C-C_h^{i+1})\big)\,d\mathbf{x}.
\end{aligned} \tag{85}
$$

Using Holder inequality, the last term can be bounded by

$$
\begin{aligned}
& -\int_\Omega ((\mathbf{u}-\mathbf{u}_h^{i+1})\cdot\nabla C)(C-C_h^{i+1})\,d\mathbf{x} \\
& -\int_\Omega (\mathbf{u}_h^{i+1}\cdot\nabla(C-C_h^{i+1})(C-C_h^{i+1})\,d\mathbf{x} \\
& +\frac{1}{2}\int_\Omega \operatorname{div}\mathbf{u}_h^{i+1}C_h^{i+1}(C-C_h^{i+1})\,d\mathbf{x} \\
& \le \frac{1}{2}(S_6^0|C|_{W^{1,3}(\Omega)}+\|C\|_{L^\infty(\Omega)})\left\|\mathbf{u}-\mathbf{u}_h^{i+1}\right\|_{L^2(\Omega)^d}|C-C_h^{i+1}|_{H^1(\Omega)}.
\end{aligned} \tag{86}
$$

Now, the last three terms of the right-hand side of (82) can be straightforwardly bounded by

$$
\begin{aligned}
& \sum_{\kappa\in\mathcal{T}_h}\Big[\int_\kappa (g-g_h)(S-S_h)\,d\mathbf{x}-\frac{\alpha}{2}\sum_{e\in\partial\kappa\cap\Gamma_h^i}\int_e[\nabla C_h^{i+1}\cdot\mathbf{n}]_e(S-S_h)\,ds \\
& +\int_\kappa(\alpha\triangle C_h^{i+1}-\mathbf{u}_h^{i+1}\cdot\nabla C_h^{i+1}-\frac{1}{2}\operatorname{div}\mathbf{u}_h^{i+1}C_h^{i+1}-r_0C_h^{i+1}+g_h)(S-S_h)d\mathbf{x}\Big] \\
& \quad\le\sum_{\kappa\in\mathcal{T}_h}\Big[(\|\,\alpha\triangle C_h^{i+1}-\mathbf{u}_h^{i+1}\cdot\nabla C_h^{i+1}-\frac{1}{2}\operatorname{div}\mathbf{u}_h^{i+1}C_h^{i+1}-r_0C_h^{i+1}+g_h\,\|_{L^2(\kappa)} \\
& \quad+\|g-g_h\|_{L^2(\kappa)})\,\|\,S-S_h\,\|_{L^2(\kappa)} \\
& \quad+\frac{1}{2}\sum_{e\in\partial\kappa\cap\Gamma_h^i}\|\,\alpha[\nabla C_h^{i+1}\cdot\mathbf{n}]\,\|_{L^2(e)}\|\,S-S_h\,\|_{L^2(e)}\Big].
\end{aligned} \tag{87}
$$

Then the fact that $S_h = R_h(S)$, the approximation properties of R_h, equations (86) and (87), and the regularity of $\mathcal{T}_h$ yield (by using the discrete Cauchy-Schwarz inequality for the equation (87))

$$
\begin{aligned}
\alpha|C-C_h^{i+1}|_{H^1(\Omega)} & \le c_1\Big(\sum_{\kappa\in\mathcal{T}_h}\big((\eta_{\kappa,i}^{(D_1)})^2+h_\kappa^2\,\|\,g-g_h\,\|_{L^2(\kappa)}^2\,\big)\Big)^{\frac{1}{2}} \\
& \quad+\frac{1}{2}(S_6^0|C|_{W^{1,3}(\Omega)}+\|C\|_{L^\infty(\Omega)})\left\|\mathbf{u}-\mathbf{u}_h^{i+1}\right\|_{L^2(\Omega)^d} \\
& \le c_1'\Big(\sum_{\kappa\in\mathcal{T}_h}\big(\eta_{\kappa,i}^{(D_1)}+h_\kappa\,\|\,g-g_h\,\|_{L^2(\kappa)}\,\big)\Big) \\
& \quad+\frac{1}{2}(S_6^0|C|_{W^{1,3}(\Omega)}+\|C\|_{L^\infty(\Omega)})\left\|\mathbf{u}-\mathbf{u}_h^{i+1}\right\|_{L^2(\Omega)^d}.
\end{aligned} \tag{88}
$$

Next, we focus on the velocity equation. The velocity error equation (65) can be written as

$$
\begin{aligned}
&\frac{\mu}{\rho}\int_\Omega K^{-1}(\mathbf{u}-\mathbf{u}_h^{i+1})\cdot\mathbf{v}\,d\mathbf{x}+\frac{\beta}{\rho}\int_\Omega(|\mathbf{u}|\mathbf{u}-|\mathbf{u}_h^{i+1}|\mathbf{u}_h^{i+1})\cdot\mathbf{v}\,d\mathbf{x}\\
&\quad+\int_\Omega\nabla(p-p_h^{i+1})\cdot\mathbf{v}\,d\mathbf{x}\\
&\quad=-\frac{\beta}{\rho}\int_\Omega\big((|\mathbf{u}_h^{i+1}|-|\mathbf{u}_h^i|)\mathbf{u}_h^{i+1}\big)\cdot\mathbf{v}\,d\mathbf{x}+\gamma\int_\Omega(\mathbf{u}_h^{i+1}-\mathbf{u}_h^i)\cdot\mathbf{v}\,d\mathbf{x}\\
&\quad+\sum_{\kappa\in\mathcal{T}_h}\Big[\int_\kappa\big(-\nabla p_h^{i+1}-\gamma(\mathbf{u}_h^{i+1}-\mathbf{u}_h^i)-\frac{\mu}{\rho}K^{-1}\mathbf{u}_h^{i+1}\\
&\quad-\frac{\beta}{\rho}|\mathbf{u}_h^i|\mathbf{u}_h^{i+1}+\mathbf{f}_h(C_h^i)\big)\cdot(\mathbf{v}-\mathbf{v}_h)\,d\mathbf{x}\\
&\quad+\int_\kappa\big(\mathbf{f}(.,C)-\mathbf{f}_h(C)\big)\cdot\mathbf{v}\,d\mathbf{x}+\int_\kappa\big(\mathbf{f}_h(C)-\mathbf{f}_h(C_h^i)\big)\cdot\mathbf{v}\,d\mathbf{x}\\
&\quad+\int_\kappa\big(\mathbf{f}_h(C_h^i)-\mathbf{f}(.,C_h^i)\big)\cdot\mathbf{v}_h\,d\mathbf{x}\Big].
\end{aligned}
\tag{89}
$$

To simplify, we set $\mathbf{z}_0=\mathbf{u}-\mathbf{u}_h^{i+1}-\mathbf{v}_r$ and we test (89) with $\mathbf{v}=\mathbf{z}_0$ and $\mathbf{v}_h=\mathbf{0}$. By construction, (76) and (66) with $q_h=r_hq$ imply that

$$
\forall q\in M,\qquad \int_\Omega\nabla q\cdot\mathbf{z}_0\,d\mathbf{x}=0. \tag{90}
$$

Hence, (89) becomes

$$
\begin{aligned}
&\frac{\mu}{\rho}\int_\Omega K^{-1}\mathbf{z}_0\cdot\mathbf{z}_0\,d\mathbf{x}+\frac{\mu}{\rho}\int_\Omega K^{-1}\mathbf{v}_r\cdot\mathbf{z}_0\,d\mathbf{x}\\
&\quad+\frac{\beta}{\rho}\int_\Omega(|\mathbf{u}|\mathbf{u}-|\mathbf{u}_h^{i+1}|\mathbf{u}_h^{i+1})(\mathbf{u}-\mathbf{u}_h^{i+1})\,d\mathbf{x}-\frac{\beta}{\rho}\int_\Omega(|\mathbf{u}|\mathbf{u}-|\mathbf{u}_h^{i+1}|\mathbf{u}_h^{i+1})\cdot\mathbf{v}_r\,d\mathbf{x}\\
&\quad=\gamma\int_\Omega(\mathbf{u}_h^{i+1}-\mathbf{u}_h^i)\cdot\mathbf{z}_0\,d\mathbf{x}-\frac{\beta}{\rho}\int_\Omega\big((|\mathbf{u}_h^{i+1}|-|\mathbf{u}_h^i|)\mathbf{u}_h^{i+1}\big)\cdot\mathbf{z}_0\,d\mathbf{x}\\
&\quad+\sum_{\kappa\in\mathcal{T}_h}\Big[\int_\kappa\big(-\nabla p_h^{i+1}-\gamma(\mathbf{u}_h^{i+1}-\mathbf{u}_h^i)\\
&\quad-\frac{\mu}{\rho}K^{-1}\mathbf{u}_h^{i+1}-\frac{\beta}{\rho}|\mathbf{u}_h^i|\mathbf{u}_h^{i+1}+\mathbf{f}_h(C_h^i)\big)\cdot\mathbf{z}_0\,d\mathbf{x}\\
&\quad+\int_\kappa\big(\mathbf{f}(.,C)-\mathbf{f}_h(C)\big)\cdot\mathbf{z}_0\,d\mathbf{x}+\int_\kappa\big(\mathbf{f}_h(C)-\mathbf{f}_h(C_h^i)\big)\cdot\mathbf{z}_0\,d\mathbf{x}\Big].
\end{aligned}
\tag{91}
$$

We decompose the fourth term in the last equation as follows

$$
\begin{aligned}
&\frac{\beta}{\rho}\int_\Omega(|\mathbf{u}|\mathbf{u}-|\mathbf{u}_h^{i+1}|\mathbf{u}_h^{i+1})\cdot\mathbf{v}_r\,d\mathbf{x}\\
&\quad=\frac{\beta}{\rho}\int_\Omega|\mathbf{u}|(\mathbf{u}-\mathbf{u}_h^{i+1})\cdot\mathbf{v}_r\,d\mathbf{x}+\frac{\beta}{\rho}\int_\Omega(|\mathbf{u}|-|\mathbf{u}_h^{i+1}|)\mathbf{u}_h^{i+1}\cdot\mathbf{v}_r\,d\mathbf{x}.
\end{aligned}
$$

Thus, equation (91) becomes by inserting $\pm\mathbf{u}$ in the second term of the right-hand side, and by using the monotonicity of $\mathcal{A}$

$$
\begin{aligned}
&\frac{\mu}{\rho}\int_\Omega K^{-1}\mathbf{z}_0\cdot\mathbf{z}_0\,d\mathbf{x} + c_m\left\|\mathbf{u}-\mathbf{u}_h^{i+1}\right\|^3_{L^3(\Omega)^d}\\
&\le \frac{\mu}{\rho}\int_\Omega |K^{-1}\mathbf{v}_r||\mathbf{z}_0|\,d\mathbf{x} + \frac{\beta}{\rho}\int_\Omega |\mathbf{u}||\mathbf{u}-\mathbf{u}_h^{i+1}||\mathbf{v}_r|\,d\mathbf{x}\\
&+\frac{\beta}{\rho}\int_\Omega |\mathbf{u}-\mathbf{u}_h^{i+1}||\mathbf{u}_h^{i+1}||\mathbf{v}_r|\,d\mathbf{x} + \gamma\int_\Omega |\mathbf{u}_h^i-\mathbf{u}_h^{i+1}||\mathbf{z}_0|\,d\mathbf{x}\\
&+\frac{\beta}{\rho}\int_\Omega |\mathbf{u}_h^{i+1}-\mathbf{u}_h^i||\mathbf{u}_h^{i+1}-\mathbf{u}||\mathbf{z}_0|\,d\mathbf{x} + \frac{\beta}{\rho}\int_\Omega |\mathbf{u}_h^{i+1}-\mathbf{u}_h^i||\mathbf{u}||\mathbf{z}_0|\,d\mathbf{x}\\
&+\sum_{\kappa\in\mathcal{T}_h}\Big[\int_\kappa |-\nabla p_h^{i+1}-\gamma(\mathbf{u}_h^{i+1}-\mathbf{u}_h^i)\\
&-\frac{\mu}{\rho}K^{-1}\mathbf{u}_h^{i+1}-\frac{\beta}{\rho}|\mathbf{u}_h^i|\mathbf{u}_h^{i+1}+\mathbf{f}_h(C_h^i)||\mathbf{z}_0|\,d\mathbf{x}\\
&+\int_\kappa \big|\mathbf{f}(.,C)-\mathbf{f}_h(C)||\mathbf{z}_0|\,d\mathbf{x} + \int_\kappa \big|\mathbf{f}_h(C)-\mathbf{f}_h(C_h^i)\big||\mathbf{z}_0|\,d\mathbf{x}\Big].
\end{aligned}
\tag{92}
$$

By using the relation $\mathbf{u}-\mathbf{u}_h^{i+1}=\mathbf{z}_0+\mathbf{v}_r$ and applying (67), we obtain

$$
\begin{aligned}
&\frac{\mu K_m}{\rho}\|\mathbf{z}_0\|^2_{L^2(\Omega)^d} + c_m\left\|\mathbf{u}-\mathbf{u}_h^{i+1}\right\|^3_{L^3(\Omega)^d}\\
&\le \frac{\mu K_M}{\rho}\|\mathbf{v}_r\|_{L^2(\Omega)^d}\,\|\mathbf{z}_0\|_{L^2(\Omega)^d}\\
&+\frac{\beta}{\rho}\|\mathbf{u}\|_{L^6(\Omega)^d}(\|\mathbf{z}_0\|_{L^2(\Omega)^d}+\|\mathbf{v}_r\|_{L^2(\Omega)^d})\|\mathbf{v}_r\|_{L^3(\Omega)^d}\\
&+\frac{\beta}{\rho}(\|\mathbf{v}_r\|_{L^2(\Omega)^d}+\|\mathbf{z}_0\|_{L^2(\Omega)^d})\|\mathbf{u}_h^{i+1}\|_{L^6(\Omega)^d}\,\|\mathbf{v}_r\|_{L^3(\Omega)^d}\\
&+\gamma\|\mathbf{u}_h^{i+1}-\mathbf{u}_h^i\|_{L^2(\Omega)^d}\,\|\mathbf{z}_0\|_{L^2(\Omega)^d}\\
&+\frac{\beta}{\rho}\|\mathbf{u}_h^{i+1}-\mathbf{u}_h^i\|_{L^\infty(\Omega)^d}\,(\|\mathbf{v}_r\|_{L^2(\Omega)^d}+\|\mathbf{z}_0\|_{L^2(\Omega)^d})\,\|\mathbf{z}_0\|_{L^2(\Omega)^d}\\
&+\frac{\beta}{\rho}\|\mathbf{u}_h^{i+1}-\mathbf{u}_h^i\|_{L^2(\Omega)^d}\,\|\mathbf{u}\|_{L^\infty(\Omega)^d}\,\|\mathbf{z}_0\|_{L^2(\Omega)^d}\\
&+\sum_{\kappa\in\mathcal{T}_h}\|-\nabla p_h^{i+1}-\frac{\mu}{\rho}K^{-1}\mathbf{u}_h^{i+1}-\gamma(\mathbf{u}_h^{i+1}-\mathbf{u}_h^i)\\
&-\frac{\beta}{\rho}|\mathbf{u}_h^i|\mathbf{u}_h^{i+1}+\mathbf{f}_h(C_h^i)\|_{L^2(\kappa)}\,\|\mathbf{z}_0\|_{L^2(\kappa)}\\
&+\sum_{\kappa\in\mathcal{T}_h}\|\mathbf{f}(.,C)-\mathbf{f}_h(C)\|_{L^2(\kappa)}\|\mathbf{z}_0\|_{L^2(\kappa)} + \sum_{\kappa\in\mathcal{T}_h}c_{\mathbf{f}_1}\|C-C_h^i\|_{L^2(\kappa)}\|\mathbf{z}_0\|_{L^2(\kappa)}.
\end{aligned}
\tag{93}
$$

Lemma 4.1 ensures that there exists an integer i_0 depending on h such that $\forall i\ge i_0$, $\mathbf{u}_h^{i+1}$ is bounded in $L^6(\Omega)^d$. Furthermore, we shall use the following inverse inequality

$$\|\mathbf{u}_h^{i+1}-\mathbf{u}_h^i\|_{L^\infty(\Omega)^d}\le c_I h^{-d/2}\|\mathbf{u}_h^{i+1}-\mathbf{u}_h^i\|_{L^2(\Omega)^d},$$

and the convergence of the sequence $\mathbf{u}_h^i$ to $\mathbf{u}_h$ in $L^2(\Omega)^d$ to deduce that we can chose i_0 sufficiently large so that $\|\mathbf{u}_h^{i+1}-\mathbf{u}_h^i\|_{L^2(\Omega)^d}\le h^{d/2}\mu K_m/2\beta c_I$, and then $\left\|\mathbf{u}_h^{i+1}-\mathbf{u}_h^i\right\|_{L^\infty(\Omega)^d}\le \dfrac{\mu K_m}{2\beta}$. Therefore, equation (93) becomes by inserting C_h^{i+1}

to the last term

(94)
$$\begin{aligned}
&\frac{\mu K_m}{2\rho}\|\mathbf{z}_0\|^2_{L^2(\Omega)^d} + c_m \left\|\mathbf{u}-\mathbf{u}_h^{i+1}\right\|^3_{L^3(\Omega)^d}\\
&\quad\le \frac{\mu K_M}{\rho}\|\mathbf{v}_r\|_{L^2(\Omega)^d}\,\|\mathbf{z}_0\|_{L^2(\Omega)^d} + \frac{\beta}{\rho}\|\mathbf{u}\|_{L^6(\Omega)^d}(\|\mathbf{z}_0\|_{L^2(\Omega)^d}\\
&\quad + \|\mathbf{v}_r\|_{L^2(\Omega)^d})\|\mathbf{v}_r\|_{L^3(\Omega)^d}\\
&\quad + \frac{\beta}{\rho}\hat{c_1}(\mathbf{u},p,C)(\|\mathbf{v}_r\|_{L^2(\Omega)^d} + \|\mathbf{z}_0\|_{L^2(\Omega)^d})\|\mathbf{v}_r\|_{L^3(\Omega)^d}\\
&\quad + \gamma\|\mathbf{u}_h^{i+1}-\mathbf{u}_h^i\|_{L^2(\Omega)^d}\,\|\mathbf{z}_0\|_{L^2(\Omega)^d} + \frac{\mu K_m}{2\rho}\,\|\mathbf{v}_r\|_{L^2(\Omega)^d}\,\|\mathbf{z}_0\|_{L^2(\Omega)^d}\\
&\quad + \frac{\beta}{\rho}\|\mathbf{u}_h^{i+1}-\mathbf{u}_h^i\|_{L^2(\Omega)^d}\,\|\mathbf{u}\|_{L^\infty(\Omega)^d}\,\|\mathbf{z}_0\|_{L^2(\Omega)^d}\\
&\quad + \sum_{\kappa\in\mathcal{T}_h}\|-\nabla p_h^{i+1} - \frac{\mu}{\rho}K^{-1}\mathbf{u}_h^{i+1} - \gamma(\mathbf{u}_h^{i+1}-\mathbf{u}_h^i)\\
&\quad - \frac{\beta}{\rho}|\mathbf{u}_h^i|\mathbf{u}_h^{i+1} + \mathbf{f}_h(C_h^i)\|_{L^2(\kappa)}\,\|\mathbf{z}_0\|_{L^2(\kappa)}\\
&\quad + \sum_{\kappa\in\mathcal{T}_h}\|\mathbf{f}(.,C)-\mathbf{f}_h(C)\|_{L^2(\kappa)}\,\|\mathbf{z}_0\|_{L^2(\kappa)}\\
&\quad + \sum_{\kappa\in\mathcal{T}_h} c_{\mathbf{f}_1}\|C_h^{i+1}-C_h^i\|_{L^2(\kappa)}\|\mathbf{z}_0\|_{L^2(\kappa)}\\
&\quad + \sum_{\kappa\in\mathcal{T}_h} c_{\mathbf{f}_1}\|C-C_h^{i+1}\|_{L^2(\kappa)}\|\mathbf{z}_0\|_{L^2(\kappa)}.
\end{aligned}$$

We use the decomposition $ab \le \frac{1}{2\varepsilon}a^2 + \frac{\varepsilon}{2}b^2$ for all the terms containing $\|\mathbf{z}_0\|_{L^2(\Omega)^d}$ in the right-hand side of the previous equation with ε sufficiently small so that all the terms of $\|\mathbf{z}_0\|_{L^2(\Omega)^d}$ will be dominated by the left-hand side. Then by using the inequality $\|\mathbf{v}_r\|_{L^2(\Omega)^d} \le |\Omega|^{1/6}\|\mathbf{v}_r\|_{L^3(\Omega)^d}$, the regularity of $\mathcal{T}_h$, and by taking the square root of the inequality, the following bound holds

(95)
$$\begin{aligned}
&\|\,\mathbf{z}_0\,\|_{L^2(\Omega)^d} + c_m \left\|\mathbf{u}-\mathbf{u}_h^{i+1}\right\|^{3/2}_{L^3(\Omega)^d}\\
&\quad\le \tilde{c}\Big(\|\,\mathbf{v}_r\,\|_{L^3(\Omega)^d} + \sum_{\kappa\in\mathcal{T}_h}\|\,\mathbf{u}_h^{i+1}-\mathbf{u}_h^i\,\|_{L^2(\kappa)}\\
&\quad + \sum_{\kappa\in\mathcal{T}_h}\|\nabla p_h^{i+1} + \frac{\mu}{\rho}K^{-1}\mathbf{u}_h^{i+1} + \gamma(\mathbf{u}_h^{i+1}-\mathbf{u}_h^i) + \frac{\beta}{\rho}|\mathbf{u}_h^i|\mathbf{u}_h^{i+1} - \mathbf{f}_h(C_h^i)\|_{L^2(\kappa)}\\
&\quad + \sum_{\kappa\in\mathcal{T}_h}\|\,\mathbf{f}(.,C)-\mathbf{f}_h(C)\,\|_{L^2(\kappa)} + \sum_{\kappa\in\mathcal{T}_h}||C_h^{i+1}-C_h^i||_{H^1(\kappa)}\Big)\\
&\quad + \sqrt{\frac{\rho}{\mu K_m}}S_2^0 c_{\mathbf{f}_1}|C-C_h^{i+1}|_{H^1(\Omega)},
\end{aligned}$$

where $\tilde{c}$ is a constant depending on the exact solution.

Thus, we deduce from the relation $\mathbf{u}-\mathbf{u}_h^{i+1} = \mathbf{z}_0 + \mathbf{v}_r$, the triangle inequality $\|\,\mathbf{u}-\mathbf{u}_h^{i+1}\,\|_{L^2(\Omega)^d} \le \|\,\mathbf{u}-\mathbf{u}_h^{i+1}-\mathbf{v}_r\,\|_{L^2(\Omega)^d} + \|\,\mathbf{v}_r\,\|_{L^2(\Omega)^d}$, using relations (95) and

(77), and the following inequality:

$$
\begin{aligned}
&\| \mathbf{u} - \mathbf{u}_h^{i+1} \|_{L^2(\Omega)^d} \\
&\le \tilde{c}\Big(\sum_{\kappa\in\mathcal{T}_h} \big(\eta_{\kappa,i}^{(D_3)} + \eta_{\kappa,i}^{(L_1)} + \eta_{\kappa,i}^{(L_2)} + \eta_{\kappa,i}^{(D_2)} + \| \mathbf{f}(.,C) - \mathbf{f}_h(C) \|_{L^2(\kappa)} \big)\Big) \\
&+ \sqrt{\frac{\rho}{\mu K_m}} S_2^0 c_{\mathbf{f}_1} |C - C_h^{i+1}|_{H^1(\Omega)}.
\end{aligned} \tag{96}
$$

When substituted into (88), this estimate for the velocity error gives

$$
\begin{aligned}
&\Big(\alpha - \frac{1}{2}\big(S_6^0 |C|_{W^{1,3}(\Omega)} + \| C \|_{L^\infty(\Omega)} \big)\sqrt{\frac{\rho}{\mu K_m}} S_2^0 c_{\mathbf{f}_1}\Big)|C - C_h^{i+1}|_{H^1(\Omega)} \\
&\le \tilde{c_2}\Big(\sum_{\kappa\in\mathcal{T}_h} \big(\eta_{\kappa,i}^{(D_1)} + \eta_{\kappa,i}^{(D_2)} + \eta_{\kappa,i}^{(D_3)} \\
&+ \eta_{\kappa,i}^{(L_1)} + \eta_{\kappa,i}^{(L_2)} + h_k \| g - g_h \|_{L^2(\kappa)} + \| \mathbf{f}(.,C) - \mathbf{f}_h(C) \|_{L^2(\kappa)} \big)\Big).
\end{aligned} \tag{97}
$$

In view of (80), the concentration estimate in (81) follows from (97), and in turn, the velocity estimate follows by substituting (97) into (96). □

Remark 4.4. *We mention that the previous theorem gives the upper bound of the error under the smallness condition of the exact concentration C (see relation*(80)*). Furthermore, we note that the constant appearing the upper bound* (81) *(in Theorem 4.3) is non-computable, but this fact does not affect the adaptive mesh method (in the numerical simulations section) which uses only the definition of the indicators.*

Remark 4.5. *Similarly to Theorem 3.12 in* [35]*, the last theorem gives an upper bound for the error $\mathbf{u} - \mathbf{u}_h^{i+1}$ in $L^2(\Omega)^d$. But unfortunately, it gives an upper bound of $\|\mathbf{u} - \mathbf{u}_h^{i+1}\|_{L^3(\Omega)^d}$ with the indicators to the power of* $2/3$ *(see relation* (95)*).*

Let us now show the upper bound of the error of the pressure:

Theorem 4.6. *We retain the assumptions of Theorem 4.3. There exists a positive real number i_1 depending on h such that $\forall i \ge i_1$, we have the following bound*

$$
\begin{aligned}
\| \nabla(p - p_h^{i+1}) \|_{L^{3/2}(\Omega)^d} &\le \tilde{c_1}\Big(\sum_{\kappa\in\mathcal{T}_h} \big(\eta_{\kappa,i}^{(D_1)} + \eta_{\kappa,i}^{(D_2)} + \eta_{\kappa,i}^{(D_3)} + \eta_{\kappa,i}^{(L_1)} \\
&+ \eta_{\kappa,i}^{(L_2)} + h_k \| g - g_h \|_{L^2(\kappa)} + \| \mathbf{f}(.,C) - \mathbf{f}_h(C) \|_{L^2(\kappa)} \big)\Big).
\end{aligned} \tag{98}
$$

Proof. Let $(\mathbf{u}, p, C)$ and $(\mathbf{u}_h^{i+1}, p_h^{i+1}, C_h^{i+1})$ be the respective solutions of (V_a) and (V_{ahi}). We test equation (65) with $\mathbf{v}_h = \mathbf{0}$ to get

$$
\begin{aligned}
&\int_\Omega \nabla(p - p_h^{i+1}) \cdot \mathbf{v}\, d\mathbf{x} \\
&= -\frac{\mu}{\rho} \int_\Omega K^{-1}(\mathbf{u} - \mathbf{u}_h^{i+1}) \cdot \mathbf{v}\, d\mathbf{x} - \frac{\beta}{\rho}\int_\Omega (|\mathbf{u}|\mathbf{u} - |\mathbf{u}_h^i|\mathbf{u}_h^{i+1}) \cdot \mathbf{v}\, d\mathbf{x} \\
&+ \sum_{\kappa\in\mathcal{T}_h} \Big[\int_\kappa \big(- \nabla p_h^{i+1} - \gamma(\mathbf{u}_h^{i+1} - \mathbf{u}_h^i) - \frac{\mu}{\rho} K^{-1}\mathbf{u}_h^{i+1} - \frac{\beta}{\rho}|\mathbf{u}_h^i|\mathbf{u}_h^{i+1} + \mathbf{f}_h(C_h^i)\big) \cdot \mathbf{v}\, d\mathbf{x} \\
&+ \gamma \int_\kappa (\mathbf{u}_h^{i+1} - \mathbf{u}_h^i) \cdot \mathbf{v}\, d\mathbf{x} + \int_\kappa \big(\mathbf{f}(.,C) - \mathbf{f}_h(C)\big) \cdot \mathbf{v}\, d\mathbf{x} \\
&+ \int_\kappa \big(\mathbf{f}_h(C) - \mathbf{f}_h(C_h^i)\big) \cdot \mathbf{v}\, d\mathbf{x}\Big],
\end{aligned} \tag{99}
$$

By using the Cauchy-Schwarz inequality, we get

(100)
$$\begin{aligned}
&\Big|\int_\Omega \nabla(p_h^{i+1}-p)\mathbf{v}\,d\mathbf{x}\Big| \le c(||\mathbf{u}-\mathbf{u}_h^{i+1}||_{L^2(\Omega)^d}+||\mathbf{u}_h^i-\mathbf{u}_h^{i+1}||_{L^2(\Omega)^d})||\mathbf{v}||_{L^2(\Omega)^d}\\
&+c_1\Big(\sum_{\kappa\in\mathcal{T}_h}||\mathbf{f}(.,C)-\mathbf{f}_h(C)||^2_{L^2(\kappa)}\Big)^{1/2}||\mathbf{v}||_{L^2(\Omega)^d}+\frac{\beta}{\rho}\Big|\int_\Omega(|\mathbf{u}|\mathbf{u}-|\mathbf{u}_h^i|\mathbf{u}_h^{i+1})\cdot\mathbf{v}\,d\mathbf{x}\Big|\\
&+c_2\Big(\sum_{\kappa\in\mathcal{T}_h}||-\nabla p_h^{i+1}-\gamma(\mathbf{u}_h^i-\mathbf{u}_h^{i+1})-\frac{\mu}{\rho}K^{-1}\mathbf{u}_h^{i+1}\\
&-\frac{\beta}{\rho}|\mathbf{u}_h^i|\mathbf{u}_h^{i+1}+\mathbf{f}_h(C_h^i)||^2_{L^2(\kappa)}\Big)^{1/2}||\mathbf{v}||_{L^2(\Omega)^d}\\
&+c_3\Big(\sum_{\kappa\in\Gamma_h}\parallel C-C_h^i\parallel^2_{L^2(\kappa)}\Big)^{1/2}||\mathbf{v}||_{L^2(\Omega)^d}.
\end{aligned}$$

By using the relation $||\mathbf{v}||_{L^2(\Omega)^d}\le|\Omega|^{1/6}||\mathbf{v}||_{L^3(\Omega)^d}$, all the terms of the right hand side of the previous bound can be treated as in the previous theorem except the third one which can be bounded as following:

(101)
$$\begin{aligned}
\Big|(|\mathbf{u}|\mathbf{u}-|\mathbf{u}_h^i|\mathbf{u}_h^{i+1},\mathbf{v})\Big| &\le \Big|((|\mathbf{u}|-|\mathbf{u}_h^i|)\mathbf{u},\mathbf{v})\Big|+\Big|(|\mathbf{u}_h^i|(\mathbf{u}-\mathbf{u}_h^{i+1}),\mathbf{v})\Big|\\
&\le \big(||\mathbf{u}-\mathbf{u}_h^i||_{L^2(\Omega)^d}||\mathbf{u}||_{L^6(\Omega)^d}\\
&\quad+||\mathbf{u}_h^i||_{L^6(\Omega)^d}||\mathbf{u}-\mathbf{u}_h^{i+1}||_{L^2(\Omega)^d}\big)||\mathbf{v}||_{L^3(\Omega)^d}.
\end{aligned}$$

We consider equation (100). By using the following inequality

$$\parallel\mathbf{u}-\mathbf{u}_h^i\parallel_{L^2(\Omega)^d}\le\parallel\mathbf{u}-\mathbf{u}_h^{i+1}\parallel_{L^2(\Omega)^d}+\parallel\mathbf{u}_h^{i+1}-\mathbf{u}_h^i\parallel_{L^2(\Omega)^d},$$

the fact that $\parallel\mathbf{u}_h^i\parallel_{L^6(\Omega)^d}$ is bounded, the inf-sup condition (11) and Theorem 4.3, we get the desired error bound on the pressure. □

Remark 4.7. *The bounds* (81) *and* (98) *represent our a posteriori error estimates where we bound the error between the exact solution* $(\mathbf{u},p,C)$ *of* (V_a) *and the numerical solution* $(\mathbf{u}_h^{i+1},p_h^{i+1},C_h^{i+1})$ *of* (V_{ahi}) *by the indicators* $\eta_{\kappa,i}^{(L)}$, $\eta_{\kappa,i}^{(D_1)}$, $\eta_{\kappa,i}^{(D_2)}$ *and* $\eta_{\kappa,i}^{(D_3)}$. *On the other hand, to get efficiency and bound the obtained indicators which is the subject of the next subsection (Section 4.2), we need to derive an additional error estimate (classical in this kind of problems) involving the exact and the numerical solutions provided in the following theorem.*

Theorem 4.8. *Under the assumptions of Lemma 4.1 and if* $\mathbf{f}_0\in L^2(\Omega)^d$, *there exists an integer* i_0 *depending on* h *such that for all* $i\ge i_0$, *the solutions* $(\mathbf{u},p)$ *of* (V_a) *and* $(\mathbf{u}_h^{i+1},p_h^{i+1})$ *of* (V_{ahi}) *verify the following error inequality:*

(102)
$$\begin{aligned}
&\parallel\big(\frac{\beta}{\rho}(|\mathbf{u}|\mathbf{u}-|\mathbf{u}_h^i|\mathbf{u}_h^{i+1})+\nabla(p-p_h^{i+1})\big)\parallel_{L^2(\Omega)^d}\\
&\le\tilde{c_2}\Big(\sum_{\kappa\in\mathcal{T}_h}\big(\eta_{\kappa,i}^{(D_1)}+\eta_{\kappa,i}^{(D_2)}+\eta_{\kappa,i}^{(D_3)}+\eta_{\kappa,i}^{(L_1)}\\
&\quad+\eta_{\kappa,i}^{(L_2)}+h_k\parallel g-g_h\parallel_{L^2(\kappa)}+\parallel\mathbf{f}(.,C)-\mathbf{f}_h(C)\parallel_{L^2(\kappa)}\big)\Big)
\end{aligned}$$

where $\tilde{c_2}>0$ *is a constant independent of* h.

Proof. Using the fact that $\mathbf{u}\in L^\infty(\Omega)^d$, then the first equation of system (P) allows us to get $\nabla p\in L^2(\Omega)^d$. Thus, the velocity error equation (65) is valid for all $\mathbf{v}$ in

$L^2(\Omega)^d$, and can be written as:

$$\begin{aligned}
&\int_\Omega \big(\frac{\beta}{\rho}(|\mathbf{u}|\mathbf{u} - |\mathbf{u}_h^i|\mathbf{u}_h^{i+1}) + \nabla(p - p_h^{i+1})\big) \cdot \mathbf{v}\, d\mathbf{x} \\
&= -\frac{\mu}{\rho}\int_\Omega K^{-1}(\mathbf{u} - \mathbf{u}_h^{i+1}) \cdot \mathbf{v}\, d\mathbf{x} \\
&+ \sum_{\kappa\in\mathcal{T}_h} \Big[\int_\kappa \big(- \nabla p_h^{i+1} - \gamma(\mathbf{u}_h^{i+1} - \mathbf{u}_h^i) \\
&- \frac{\mu}{\rho}K^{-1}\mathbf{u}_h^{i+1} - \frac{\beta}{\rho}|\mathbf{u}_h^i|\mathbf{u}_h^{i+1} + \mathbf{f}_h(C_h^i)\big) \cdot (\mathbf{v} - \mathbf{v}_h)\, d\mathbf{x} \\
&+ \gamma\int_\kappa (\mathbf{u}_h^{i+1} - \mathbf{u}_h^i) \cdot \mathbf{v}\, d\mathbf{x} + \int_\kappa \big(\mathbf{f}(.,C) - \mathbf{f}_h(C)\big) \cdot \mathbf{v}\, d\mathbf{x} \\
&+ \int_\kappa \big(\mathbf{f}_h(C) - \mathbf{f}_h(C_h^i)\big) \cdot \mathbf{v}\, d\mathbf{x} + \int_\kappa \big(\mathbf{f}_h(C_h^i) - \mathbf{f}(.,C_h^i)\big) \cdot \mathbf{v}_h\, d\mathbf{x}\Big],
\end{aligned} \tag{103}$$

By taking $\mathbf{v}_h = \mathbf{0}$ and $\mathbf{v} = \big(\frac{\beta}{\rho}(|\mathbf{u}|\mathbf{u} - |\mathbf{u}_h^i|\mathbf{u}_h^{i+1}) + \nabla(p - p_h^{i+1})\big)$, applying the Cauchy-Schwarz inequality and simplifying by $\|\mathbf{v}\|_{L^2(\Omega)^d}$, we get the result by using Theorem 4.3.

4.2. Lower error bound. *In order to establish the efficiency of the a posteriori error estimates, we recall the following properties (see R. Verfürth,*[40]*, Chapter 1). For an element κ of $\mathcal{T}_h$, we consider the bubble function ψ_κ (resp. ψ_e for the face e) which is equal to the product of the $d+1$ barycentric coordinates associated with the vertices of κ (resp. of the d barycentric coordinates associated with the vertices of e). We also consider a lifting operator $\mathcal{L}_e$ defined on polynomials on e vanishing on ∂e into polynomials on the at most two elements κ containing e and vanishing on $\partial\kappa \setminus e$, which is constructed by affine transformation from a fixed operator on the reference element.*

Property 4.9. *Denoting by $Pr(\kappa)$ the space of polynomials of degree smaller than r on κ. The following properties hold:*

$$\forall v \in P_r(\kappa), \qquad \begin{cases} c||v||_{0,\kappa} \le ||v\psi_\kappa^{1/2}||_{0,\kappa} \le c'||v||_{0,\kappa}, \\ |v|_{1,\kappa} \le ch_\kappa^{-1}||v||_{0,\kappa}. \end{cases} \tag{104}$$

Property 4.10. *Denoting by $Pr(e)$ the space of polynomials of degree smaller than r on e, we have*

$$\forall\, v \in P_r(e), \qquad c\|v\|_{0,e} \le \|v\psi_e^{1/2}\|_{0,e} \le c'\|v\|_{0,e},$$

and, for all polynomials v in $Pr(e)$ vanishing on ∂e, if κ is an element which contains e,

$$\|\mathcal{L}_e v\|_{0,\kappa} + h_e \mid \mathcal{L}_e v \mid_{1,\kappa} \le ch_e^{1/2}\|v\|_{0,e}.$$

Let us start with the concentration errors indicators.

Theorem 4.11. *Under the assumptions of Theorem 3.4 and Lemma 4.1, for all $\kappa \in \mathcal{T}_h$ we have:*

$$\eta_{\kappa,i}^{(D_1)} \le c\big(\|\mathbf{u}_h^{i+1} - \mathbf{u}\|_{L^2(w_e)} + \|C - C_h^{i+1}\|_{H^1(w_e)} + \sum_{\kappa\subset w_e} h_\kappa \|g - g_h\|_{L^2(\kappa)} \big) \tag{105}$$

where c is a positive constant depending on the exact solution but independent of h and w_k. Moreover, without any assumption we have:

$$\eta_{\kappa,i}^{(L_2)} \le \|C - C_h^{i+1}\|_{H^1(\kappa)} + \|C - C_h^i\|_{H^1(\kappa)}. \tag{106}$$

Proof. The bound (106) is obvious using a triangular inequality. In order to derive a lower bound for the interior part of $\eta_{\kappa,i}^{(D_1)}$, we start from equation (64). By using that $\operatorname{div}\mathbf{u} = 0$ and applying Green's formula, the term $-\frac{1}{2}\int_\Omega \operatorname{div}\mathbf{u}_h^{i+1} C_h^{i+1} S\, d\mathbf{x}$ can be written as:

$$
\begin{aligned}
&-\frac{1}{2}\int_\Omega \operatorname{div}\mathbf{u}_h^{i+1} C_h^{i+1} S\, d\mathbf{x}\\
&= -\frac{1}{2}\int_\Omega \operatorname{div}(\mathbf{u}_h^{i+1}-\mathbf{u}) C_h^{i+1} S\, d\mathbf{x}\\
&= -\frac{1}{2}\int_\Omega \operatorname{div}(\mathbf{u}_h^{i+1}-\mathbf{u})(C_h^{i+1}-R_h(C)) S\, d\mathbf{x}\\
&-\frac{1}{2}\int_\Omega \operatorname{div}(\mathbf{u}_h^{i+1}-\mathbf{u}) R_h(C) S\, d\mathbf{x}\\
&= \frac{1}{2}\int_\Omega (\mathbf{u}_h^{i+1}-\mathbf{u})\cdot\nabla(C_h^{i+1}-R_h(C)) S\, d\mathbf{x}\\
&+\frac{1}{2}\int_\Omega (\mathbf{u}_h^{i+1}-\mathbf{u})\cdot\nabla S(C_h^{i+1}-R_h(C))\, d\mathbf{x}\\
&+\frac{1}{2}\int_\Omega (\mathbf{u}_h^{i+1}-\mathbf{u})\cdot((\nabla R_h(C))S+(\nabla S)R_h(C))\, d\mathbf{x}.
\end{aligned}
\tag{107}
$$

In view of (107), by taking $S_h = 0$ and $S = S_\kappa$, where in each element κ, S_κ is the localizing function:

$$
S_\kappa = \big(\alpha\triangle C_h^{i+1} - \mathbf{u}_h^{i+1}\cdot\nabla C_h^{i+1} - \frac{1}{2}\operatorname{div}\mathbf{u}_h^{i+1} C_h^{i+1} - r_0 C_h^{i+1} + g_h\big)\psi_\kappa,
\tag{108}
$$

extended by 0 outside κ, hence equation (64) becomes:

$$
\begin{aligned}
&\int_\kappa (\alpha\triangle C_h^{i+1} - \mathbf{u}_h^{i+1}\cdot\nabla C_h^{i+1} - \frac{1}{2}\operatorname{div}\mathbf{u}_h^{i+1} C_h^{i+1} - r_0 C_h^{i+1} + g_h)^2\psi_\kappa\, d\mathbf{x}\\
&= \alpha\int_\kappa \nabla(C - C_h^{i+1})\cdot\nabla S_\kappa\, d\mathbf{x} + r_0\int_\kappa (C - C_h^{i+1}) S_\kappa\, d\mathbf{x}\\
&+\int_\kappa ((\mathbf{u}-\mathbf{u}_h^{i+1})\cdot\nabla C) S_\kappa\, d\mathbf{x} + \int_\kappa (\mathbf{u}_h^{i+1}\cdot\nabla(C - C_h^{i+1})) S_\kappa\, d\mathbf{x}\\
&-\int_\kappa (g - g_h) S_\kappa\, d\mathbf{x} + \frac{1}{2}\int_\kappa (\mathbf{u}_h^{i+1}-\mathbf{u})\cdot\nabla(C_h^{i+1}-R_h(C)) S_\kappa\, d\mathbf{x}\\
&+\frac{1}{2}\int_\kappa (\mathbf{u}_h^{i+1}-\mathbf{u})\cdot\nabla S_\kappa(C_h^{i+1}-R_h(C))\, d\mathbf{x}\\
&+\frac{1}{2}\int_\kappa (\mathbf{u}_h^{i+1}-\mathbf{u})\cdot((\nabla R_h(C))S_\kappa+(\nabla S_\kappa)R_h(C))\, d\mathbf{x}.
\end{aligned}
\tag{109}
$$

In order to bound the right-hand-side of the previous equation, we start by bounding the last three terms as following:

$$
\begin{aligned}
&\frac{1}{2}\int_\kappa (\mathbf{u}_h^{i+1}-\mathbf{u})\cdot\nabla(C_h^{i+1}-R_h(C))S_\kappa\,d\mathbf{x}\\
&+\frac{1}{2}\int_\kappa (\mathbf{u}_h^{i+1}-\mathbf{u})\cdot\nabla S_\kappa(C_h^{i+1}-R_h(C))\,d\mathbf{x}\\
&+\frac{1}{2}\int_\kappa (\mathbf{u}_h^{i+1}-\mathbf{u})\cdot((\nabla R_h(C))S_\kappa+(\nabla S_\kappa)R_h(C))\,d\mathbf{x}\\
&\le \frac{1}{2}\left\|\mathbf{u}-\mathbf{u}_h^{i+1}\right\|_{L^2(\kappa)}\big(c_I(6)c_I(3)h_\kappa^{-d/2}|C_h^{i+1}-R_h(C)|_{H^1(\kappa)}\\
&+c_I(3)c_L h_\kappa^{(-d-6)/6}\left\|C_h^{i+1}-R_h(C)\right\|_{L^6(\kappa)}\\
&+c_I(6)h_\kappa^{-d/3}|R_h(C)|_{W^{1,3}(\kappa)}+c_L h_\kappa^{-1}\left\|R_h(C)\right\|_{L^\infty(\kappa)}\big)\left\|S_\kappa\right\|_{L^2(\kappa)}\\
&\le \frac{1}{2}\left\|\mathbf{u}-\mathbf{u}_h^{i+1}\right\|_{L^2(\kappa)}\big(c_I(6)c_I(3)h_\kappa^{-d/2}(|C_h^{i+1}-C_h|_{H^1(\kappa)}\\
&+|C_h-C|_{H^1(\kappa)}+|R_h(C)-C|_{H^1(\kappa)})\\
&+c_I(3)c_L h_\kappa^{(-6-d)/6}(\left\|C_h^{i+1}-C_h\right\|_{L^6(\kappa)}\\
&+\left\|C_h-C\right\|_{L^6(\kappa)}+\left\|R_h(C)-C\right\|_{L^6(\kappa)})\\
&+c_I(6)h_\kappa^{-d/3}|R_h(C)|_{W^{1,3}(\kappa)}+c_L h_\kappa^{-1}\left\|R_h(C)\right\|_{L^\infty(\kappa)}\big)\left\|S_\kappa\right\|_{L^2(\kappa)}.
\end{aligned}
\tag{110}
$$

Following Theorem 3.4 and as the sequence C_h^{i+1} converges strongly to C_h in $H^1(\Omega)$ so there exists an integer i_1 depending on h such that for all $i \ge i_1$, we have

$$
|C_h^{i+1}-C_h|_{H^1(\kappa)} \le h \qquad \text{and} \qquad \left\|C_h^{i+1}-C_h\right\|_{L^6(\kappa)} \le S_6^0 h. \tag{111}
$$

Thus, using (111), the *a priori* error estimates, the regularity properties of the operator R_h and the fact that the mesh is uniformly regular, we get:

$$
\begin{aligned}
&\frac{1}{2}\int_\kappa (\mathbf{u}_h^{i+1}-\mathbf{u})\cdot\nabla(C_h^{i+1}-R_h(C))S_\kappa\,d\mathbf{x}\\
&+\frac{1}{2}\int_\kappa (\mathbf{u}_h^{i+1}-\mathbf{u})\cdot\nabla S_\kappa(C_h^{i+1}-R_h(C))\,d\mathbf{x}\\
&+\frac{1}{2}\int_\kappa (\mathbf{u}_h^{i+1}-\mathbf{u})\cdot((\nabla R_h(C))S_\kappa+(\nabla S_\kappa)R_h(C))\,d\mathbf{x}\\
&\le \tilde{c}_1\left\|\mathbf{u}-\mathbf{u}_h^{i+1}\right\|_{L^2(\kappa)}\big(h_\kappa^{(2-d)/2}+h_\kappa^{-d/6}+h_\kappa^{-d/3}+h_\kappa^{-1}\big)\left\|S_\kappa\right\|_{L^2(\kappa)}
\end{aligned}
\tag{112}
$$

where $\tilde{c}_1$ is a positive constant depending on the exact solution but independent of h.

In view of (112), using Holder inequality, the inverse inequalities and Lemma 4.1, the left-hand-side of (109) can be bounded as follows:

$$
\begin{aligned}
&\int_\kappa (\alpha\triangle C_h^{i+1}-\mathbf{u}_h^{i+1}\cdot\nabla C_h^{i+1}-\frac{1}{2}\operatorname{div}\mathbf{u}_h^{i+1}C_h^{i+1}-r_0C_h^{i+1}+g_h)^2\psi_\kappa\,d\mathbf{x}\\
&\le \big[\alpha c_L h_\kappa^{-1}\left\|C-C_h^{i+1}\right\|_{H^1(\kappa)}+r_0\left\|C-C_h^{i+1}\right\|_{H^1(\kappa)}\\
&+c_I(6)h_\kappa^{-d/3}\left\|\mathbf{u}-\mathbf{u}_h^{i+1}\right\|_{L^2(\kappa)}|\nabla C|_{W^{1,3}(\kappa)}\\
&+\hat{c}(\mathbf{u},p,C)c_I(3)h_\kappa^{-d/6}\left\|C-C_h^{i+1}\right\|_{H^1(\kappa)}+\left\|g-g_h\right\|_{L^2(\kappa)}\\
&+\tilde{c}_1(h_\kappa^{(2-d)/2}+h_\kappa^{-d/6}+h_\kappa^{-d/3}+h_\kappa^{-1})\left\|\mathbf{u}-\mathbf{u}_h^{i+1}\right\|_{L^2(\kappa)}\big]\left\|S_\kappa\right\|_{L^2(\kappa)}.
\end{aligned}
\tag{113}
$$

We then get the bound for the first part of $\eta_{\kappa,i}^{(D_1)}$ by using Property 4.9 and multiplying the previous inequality by h_κ.

Finally, we estimate the surface part of $\eta_{\kappa,i}^{(D_1)}$ by testing (64) with $S_h = 0$ and $S = S_e$ where S_e is the localizing function defined by

$$S_e = \begin{cases} \mathcal{L}_e\big(\alpha[\nabla C_h^{i+1}\cdot \mathbf{n}]_e\psi_e\big) & \text{on } \kappa\cup\kappa', \\ 0 & \text{on } \Omega\backslash(\kappa\cup\kappa'), \end{cases}$$

and κ and κ' are the two elements adjacent to e. Then (64) reduces to

$$\begin{aligned}
&\alpha\int_e [\nabla C_h^{i+1}\cdot\mathbf{n}]_e^2\psi_e\,ds \\
&= \int_{\kappa\cup\kappa'}(\alpha\triangle C_h^{i+1} - \mathbf{u}_h^{i+1}\cdot\nabla C_h^{i+1} - \frac{1}{2}\operatorname{div}\mathbf{u}_h^{i+1}C_h^{i+1} - r_0C_h^{i+1} + g_h)S_e\,d\mathbf{x} \\
&+ \int_{\kappa\cup\kappa'}(g-g_h)S_e\,d\mathbf{x} - r_0\int_{\kappa\cup\kappa'}(C - C_h^{i+1})S_e\,d\mathbf{x} \\
&- \alpha\int_{\kappa\cup\kappa'}\nabla(C - C_h^{i+1})\cdot\nabla S_e\,d\mathbf{x} + \frac{1}{2}\int_{\kappa\cup\kappa'}\operatorname{div}\mathbf{u}_h^{i+1}C_h^{i+1}S_e\,d\mathbf{x} \\
&+ \int_{\kappa\cup\kappa'}(\mathbf{u}_h^{i+1}\cdot\nabla(C_h^{i+1} - C))S_e\,d\mathbf{x} + \int_{\kappa\cup\kappa'}((\mathbf{u}_h^{i+1} - \mathbf{u})\cdot\nabla C)S_e\,d\mathbf{x}.
\end{aligned} \tag{114}$$

In view of the continuity properties of $\mathcal{L}_e$ in Property 4.10, a bound for the above left-hand side is derived by the same arguments; for instance, by combining it with (16), we have on the elements κ sharing e:

$$\|\mathcal{L}_e(v)\|_{L^6(\kappa)} \le c c_I(6) h_\kappa^{-d/3}h_e^{1/2}\|v\|_{L^2(e)}.$$

Thus, by applying (113), we obtain

$$\begin{aligned}
&h_e^{\frac{1}{2}}\left\|\alpha[\nabla C_h^{i+1}\cdot\mathbf{n}]_e\right\|_{L^2(e)} \\
&\quad\le c\big(\left\|\mathbf{u} - \mathbf{u}_h^{i+1}\right\|_{L^2(\kappa\cup\kappa')} + |C - C_h^{i+1}|_{H^1(\kappa\cup\kappa')} + h_e\|g - g_h\|_{L^2(\kappa\cup\kappa')}\big),
\end{aligned} \tag{115}$$

which gives the desired result. □

Now, we turn to the velocity error indicators.

Theorem 4.12. *Let $(\mathbf{u}, p, C)$ and $(\mathbf{u}_h^{i+1}, p_h^{i+1}, C_h^{i+1})$ be the respective solutions to problems (V_a) and (V_{ahi}). We have the following bounds of the indicators: for each element $\kappa\in\mathcal{T}_h$,*

$$\eta_{\kappa,i}^{(L_1)} \le \left\|\mathbf{u} - \mathbf{u}_h^i\right\|_{L^2(\kappa)} + \left\|\mathbf{u} - \mathbf{u}_h^{i+1}\right\|_{L^2(\kappa)}, \tag{116}$$

and

$$\eta_{\kappa,i}^{(D_3)} \le c\|\mathbf{v}_r\|_{L^3(w_k)}, \tag{117}$$

where c is a positive constant independent of h.

Proof. The bound (116) is a simple consequence of the definition of $\eta_{\kappa,i}^{(L_1)}$ and a triangle inequality. In order to prove (117), we consider first Equation (66) with $q_h = 0$ and

$$q = q_\kappa = \begin{cases} (\operatorname{div}\mathbf{u}_h^{i+1})\psi_\kappa & \text{on } \kappa, \\ 0 & \text{on } \Omega\backslash\kappa, \end{cases}$$

where ψ_κ is the bubble functions on a given element $\kappa \in \mathcal{T}_h$. We obtain by using relation (90) the following equation:

$$\int_\kappa (\operatorname{div} \mathbf{u}_h^{i+1})^2 \psi_\kappa \, d\mathbf{x} = \int_\kappa \nabla q_k \cdot \mathbf{v}_r \, d\mathbf{x}. \tag{118}$$

Using the property 4.9, the Cauchy-Schwarz inequality, and the relation $\|\mathbf{v}\|_{L^2(\kappa)} \le |\kappa|^{1/6} \|\mathbf{v}\|_{L^3(\kappa)} \le h_\kappa^{d/6} \|\mathbf{v}\|_{L^3(\kappa)}$ lead to

$$\begin{aligned} \|\operatorname{div} \mathbf{u}_h^{i+1}\|_{L^2(\kappa)} &\le c h_\kappa^{-1} \|\mathbf{v}_r\|_{L^2(\kappa)} \\ &\le c h_\kappa^{(-6+d)/6} \|\mathbf{v}_r\|_{L^3(\kappa)}. \end{aligned} \tag{119}$$

Then we get by considering the first inverse inequality (16) with $p = 3$, and by multiplying by h_κ

$$h_\kappa \|\operatorname{div} \mathbf{u}_h^{i+1}\|_{L^3(\kappa)} \le c_2 \|\mathbf{v}_r\|_{L^3(\kappa)}, \tag{120}$$

which corresponds to the first divergence part of the indicator $\eta_{\kappa,i}^{(D_3)}$.

Again, we consider equation (66) with $q_h = 0$ and

$$q = q_e = \begin{cases} \mathcal{L}_{e,\kappa}(\phi_{h,1}^e \psi_e) & \text{on } \{\kappa, \kappa'\}, \\ 0 & \text{on } \Omega \backslash (\kappa \cup \kappa'), \end{cases}$$

where ψ_e is the bubble function of e and κ' denotes the other element of $\mathcal{T}_h$ that share e with κ. We get the following equation:

$$\int_e (\phi_{h,1}^e)^2 \psi_e \, ds = \int_{\kappa\cup\kappa'} \operatorname{div} \mathbf{u}_h^{i+1} q_e \, d\mathbf{x} - \int_{\kappa\cup\kappa'} \nabla q_e \cdot \mathbf{v}_r \, d\mathbf{x}$$

Properties 4.9 and 4.10 allow us to get the following bound:

$$\|\phi_{h,1}^e\|_{L^2(e)} \le c\big(h_e^{1/2} \|\operatorname{div} \mathbf{u}_h^{i+1}\|_{L^2(\kappa\cup\kappa')} + h_e^{-1/2} \|\mathbf{v}_r\|_{L^2(\kappa\cup\kappa')}\big).$$

By using the second inverse inequality 16, the relation $\|\mathbf{v}_h\|_{L^2(\kappa)} \le |\kappa|^{1/6} \|\mathbf{v}_h\|_{L^3(\kappa)}$, and that the family of triangulation is uniformly regular, we obtain the bound:

$$h_e^{1/3} \|\phi_{h,1}^e\|_{L^3(e)} \le c\big(h_e \|\operatorname{div} \mathbf{u}_h^{i+1}\|_{L^3(\kappa\cup\kappa')} + \|\mathbf{v}_r\|_{L^3(\kappa\cup\kappa')}\big). \tag{121}$$

Hence, we bound the part of $\eta_{\kappa,i}^{(D_3)}$ corresponding to $\phi_{h,1}^e$. Relations (120) and (121) give (117). $\square$

Theorem 4.13. *Under the assumptions of Lemma 4.1, we have the following bound*

(122)

$$\begin{aligned} \eta_{\kappa,i}^{(D_2)} \le \hat{c}\big(\eta_{\kappa,i}^{(L_1)} &+ \|\mathbf{u} - \mathbf{u}_h^{i+1}\|_{L^2(w_\kappa)} + \|\frac{\beta}{\rho}\big(|\mathbf{u}|\mathbf{u} - |\mathbf{u}_h^{i+1}|\mathbf{u}_h^{i+1}\big) + \nabla(p - p_h^{i+1})\|_{L^2(\kappa)} \\ &+ \|\mathbf{f}(.,C) - \mathbf{f}_h(C)\|_{L^2(w_\kappa)} + \|K^{-1} - K_h^{-1}\|_{L^3(w_\kappa)} + c_{\mathbf{f}_1} \|C - C_h^{i+1}\|_{H^1(w_\kappa)} \end{aligned}$$

where $\hat{c}$ is a constant independent of the mesh step but depends on the exact solution $(\mathbf{u}, p)$, and K_h^{-1} is an approximation of K^{-1} which is a constant tensor in each element.

Proof. Let us now prove relation (4.13). We consider equation (65) with $\mathbf{v}_h = 0$, and

$$\begin{aligned} \mathbf{v} =& \mathbf{v}_\kappa \\ =& \begin{cases} \big(-\nabla p_h^{i+1} - \gamma(\mathbf{u}_h^{i+1} - \mathbf{u}_h^i) - \dfrac{\mu}{\rho} K_h^{-1} \mathbf{u}_h^{i+1} - \dfrac{\beta}{\rho} |\mathbf{u}_h^i| \mathbf{u}_h^{i+1} + \mathbf{f}_h(C_h^i)\big)\psi_\kappa & \text{on } \kappa, \\ 0 \quad \text{on } \Omega\backslash\kappa. \end{cases} \end{aligned}$$

Therefore

$$\int_\kappa |(-\nabla p_h^{i+1} - \gamma(\mathbf{u}_h^{i+1} - \mathbf{u}_h^i) - \frac{\mu}{\rho} K_h^{-1}\mathbf{u}_h^{i+1} - \frac{\beta}{\rho}|\mathbf{u}_h^i|\mathbf{u}_h^{i+1} + \mathbf{f}_h(C_h^i))\psi_\kappa^{1/2}|^2 d\mathbf{x}$$
$$= \frac{\mu}{\rho}\int_\kappa (K^{-1} - K_h^{-1})\mathbf{u}_h^{i+1}\cdot \mathbf{v}\, d\mathbf{x} + \frac{\mu}{\rho}\int_\kappa K^{-1}(\mathbf{u} - \mathbf{u}_h^{i+1})\cdot \mathbf{v}\, d\mathbf{x}$$
$$+ \frac{\beta}{\rho}\int_\kappa (|\mathbf{u}|\mathbf{u} - |\mathbf{u}_h^i|\mathbf{u}_h^{i+1})\cdot \mathbf{v}\, d\mathbf{x} + \int_\kappa \nabla(p - p_h^{i+1})\cdot \mathbf{v}\, d\mathbf{x}$$
$$- \gamma\int_K (\mathbf{u}_h^{i+1} - \mathbf{u}_h^i)\cdot \mathbf{v}\, d\mathbf{x}, + \int_\kappa (\mathbf{f}(.,C) - \mathbf{f}_h(C))\cdot \mathbf{v}\, d\mathbf{x}$$
$$+ \int_\kappa (\mathbf{f}_h(C) - \mathbf{f}_h(C_h^i))\cdot \mathbf{v}\, d\mathbf{x}.$$

By using Lemma 4.1, the bound (67) and Properties 4.9-4.10, we get the following bound:

$$\begin{aligned}
&\left\| -\nabla p_h^{i+1} - \gamma(\mathbf{u}_h^{i+1} - \mathbf{u}_h^i) - \frac{\mu}{\rho}K_h^{-1}\mathbf{u}_h^{i+1} - \frac{\beta}{\rho}|\mathbf{u}_h^i|\mathbf{u}_h^{i+1} + \mathbf{f}_h(C_h^i)\right\|_{L^2(\kappa)} \\
&\le \hat{c}\big(\left\|K^{-1} - K_h^{-1}\right\|_{L^3(\kappa)} + \frac{\mu K_M}{\rho}\left\|\mathbf{u} - \mathbf{u}_h^{i+1}\right\|_{L^2(\kappa)} \\
&+ \left\| \frac{\beta}{\rho}(|\mathbf{u}|\mathbf{u} - |\mathbf{u}_h^i|\mathbf{u}_h^{i+1}) + \nabla(p - p_h^{i+1}]\right\|_{L^2(\kappa)} \\
&+ \gamma\left\|\mathbf{u}_h^{i+1} - \mathbf{u}_h^i\right\|_{L^2(\kappa)} + \|\mathbf{f}(.,C) - \mathbf{f}_h(C)\|_{L^2(\kappa)} + c_{\mathbf{f}_1}\left\|C - C_h^{i+1}\right\|_{H^1(\kappa)}\big).
\end{aligned} \tag{123}$$

Finally, we obtain the result by using the following triangle inequality, and Lemma 4.1:

$$\begin{aligned}
&\| - \nabla p_h^{i+1} - \gamma(\mathbf{u}_h^{i+1} - \mathbf{u}_h^i) - \frac{\mu}{\rho}K^{-1}\mathbf{u}_h^{i+1} - \frac{\beta}{\rho}|\mathbf{u}_h^i|\mathbf{u}_h^{i+1} + \mathbf{f}_h(C_h^i)\|_{L^2(\kappa)} \\
&\le \|\nabla p_h^{i+1} + \gamma(\mathbf{u}_h^{i+1} - \mathbf{u}_h^i) + \frac{\mu}{\rho}K_h^{-1}\mathbf{u}_h^{i+1} + \frac{\beta}{\rho}|\mathbf{u}_h^i|\mathbf{u}_h^{i+1} - \mathbf{f}_h(C_h^i)\|_{L^2(\kappa)} \\
&+ \frac{\mu}{\rho}\|K^{-1} - K_h^{-1}\|_{L^3(\kappa)}\|\mathbf{u}_h^{i+1}\|_{L^6(\kappa)}.
\end{aligned} \tag{124}$$

□

Remark 4.14. *The efficiency of the a posteriori error estimates is given by the lower bounds* (105)*,* (116)*,* (117) *and* (4.13)*. We note that the constants appearing in these lower bounds are non-computable as they depend on the constant of the a priori error estimate of Theorem 3.1.*

5. Numerical results

The main goal of this section is to validate the theoretical results of the previous sections, all numerical simulations are in two dimensions and performed using Freefem++ (see [26]*). We shall study two cases: the first one is an academic one where the numerical solution is compared to the known exact one, the second case treats the Lid-Driven cavity which is a very popular, and interesting one.*

5.1. First test case. *In this subsection, the domain* Ω *is the unit square* $]0,1[\times]0,1[$ *and all computations start on a uniform initial triangular mesh obtained by dividing the domain into* N^2 *equal squares, each one subdivided into two triangles, so that the initial triangulation consists of* $2N^2$ *triangles. We apply the numerical scheme*

(V_{ahi}) to the exact solution $(\mathbf{u}, p, C) = (\mathbf{curl}\,\psi, p, C)$ where $\psi, p,$ and C are given by

$$\psi(x,y) = e^{-\delta((x-0.5)^2+(y-0.5)^2)}, \tag{125}$$

$$p(x,y) = x(x-2/3)y(y-2/3), \tag{126}$$

and

$$C(x,y) = x^2(x-1)^2y^2(y-1)^2e^{-\delta((x-0.5)^2+(y-0.5)^2)}, \tag{127}$$

with the choice $\delta = 50; \gamma = \beta = 10; \alpha = \mu = \rho = r_0 = 1$; $K = I$ and $\mathbf{f}_1(C) = (2 + C, 2 + 2\sin(C))$. Thus, we compute $\mathbf{f}_0$ and g by using their expressions in problem (P). For the choice of the parameter γ, we refer to [35] where we compared the numerical scheme for different values of the parameter γ. In addition, we take $N = 20$ on the initial mesh.

The algorithm starts with the initial guesses $C_h^0 = 0$ and $\mathbf{u}_h^0 = u_{hd}^0$ where u_{hd}^0 is calculated using the Darcy problem which corresponds to $\beta = 0$.

The theory is tested by applying the numerical scheme (V_{ahi}) to the exact solution. For a given mesh indexed by h, we consider the total errors:

$$Err2 = \Big(\frac{||\mathbf{u}_h - \mathbf{u}||_{L^2(\Omega)} + ||\nabla(p_h - p)||_{L^{3/2}(\Omega)} + ||C_h - C||_{H^1(\Omega)}}{||\mathbf{u}||_{L^2(\Omega)} + ||\nabla p||_{L^{3/2}(\Omega)} + ||C||_{H^1(\Omega)}}\Big)$$

and

$$Err3 = \Big(\frac{||\mathbf{u}_h - \mathbf{u}||_{L^3(\Omega)} + ||\nabla(p_h - p)||_{L^{3/2}(\Omega)} + ||C_h - C||_{H^1(\Omega)}}{||\mathbf{u}||_{L^3(\Omega)} + ||\nabla p||_{L^{3/2}(\Omega)} + ||C||_{H^1(\Omega)}}\Big),$$

where $(\mathbf{u}_h, p_h, C_h)$ is the numerical solution $(\mathbf{u}_h^{i+1}, p_h^{i+1}, C_h^{i+1})$ obtained by the iterative scheme (V_{ahi}) after the convergence with respect to the index i.

It should be noted that the definition of $Err2$ takes into account the error of the velocity in $L^2(\Omega)^2$ which is the norm associated to the theoretical studies of the previous sections, while the definition $Err3$ considers the error of the velocity in $L^3(\Omega)^2$ where the velocity lives. In the following, we show comparisons of $Err2$ and $Err3$ between the exact and the adaptive methods.

For the computation of the numerical solution by using the scheme (V_{ahi}), it is convenient to compute the following global indicators:

$$\eta_i^{(D)} = \Big(\sum_{K\in\mathcal{T}_h} \big((\eta_{K,i}^{(D_1)})^2 + (\eta_{K,i}^{(D_2)})^2 + (\eta_{K,i}^{(D_3)})^2\big)^{\frac{1}{2}}\Big)$$

and

$$\eta_i^{(L)} = \Big(\sum_{K\in\mathcal{T}_h} \big((\eta_{K,i}^{(L_1)})^2 + (\eta_{K,i}^{(L_2)})^2\big)^{\frac{1}{2}}\Big)$$

where the indicators $\eta_{K,i}^{(D_l)}$ and $\eta_{K,j}^{(L_j)}$ with $l \in \{1,2,3\}$ and $j \in \{1,2\}$ are given in equations (68)-(72). These indicators are used for the stopping criteria given by the relation

$$\eta_i^{(L)} \le \bar{\gamma}\eta_i^{(D)} \tag{128}$$

where $\bar{\gamma} = 0.01$. This stopping criteria was first introduced, interpreted and discussed in [18] and [20], and then used in multiple works (see for instance [35]). In fact, it balances the linearization and discretization indicators in the sense that for a given mesh, it is useless to continue the iterations if (128) is verified.

For the adaptive mesh (refinement and coarsening), we use routines in Freefem++. The indicators are used for mesh adaptation by the adapted mesh algorithm used *in* [35]*, but here we add the convection-diffusion-reaction equation and for reader's convenience, we prefered to recall the algorithm:*

(1) *Given* $(\mathbf{u}_h^i, C_h^i)$*,*
   (a) *Solve the problem* (V_{ahi}) *to compute* $(\mathbf{u}_h^{i+1}, p_h^{i+1}, C_h^{i+1})$*.*
   (b) *Calculate* $\eta_i^{(D)}$ *and* $\eta_i^{(L)}$*.*

(2) *If the stopping criterion* (128) *is satisfied, go to (3), else set* $\mathbf{u}_h^i = \mathbf{u}_h^{i+1}, C_h^i = C_h^{i+1}, p_h^i = p_h^{i+1}$ *and go to (1).*

(3)
   (a) *If* $\eta_i^{(D)}$ *is smaller than a fixed error tolerance* $\varepsilon = 10^{-8}$*, we stop the iterations and the algorithm.*
   (b) *Else we adapt the mesh using the indicators* $\eta_{K,i}^{(D)}$*.*

(4) *Set* $i = i + 1$ *and go to (1).*

In Figure 1, we present the evolution of the mesh during the iterations (initial, second and fifth refinement levels). We notice that the mesh is concentrated in the region where the solution needs to be well described as the velocity is a ball concentrated at the center of Ω*.*

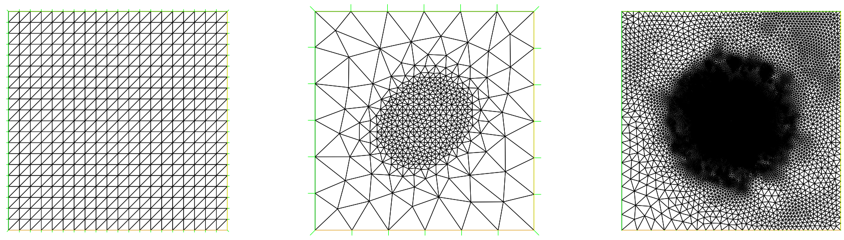

FIGURE 1. Evolution of the mesh during the refinement levels (initial, second and fifth).

Tables 1 and 2 show the rate of convergence of the errors $Err2$ *and* $Err3$ *in logarithmic scale for the uniform and adaptive methods with respect to the total number of degree of freedom (TDOF).*

TABLE 1. Uniform method: rate of the error $Err2$ and $Err3$ with respect to the total degree of freedom in logarithmic scale.

TDOF	**Err2**	**rate**
3.87	−0.95	−
4.28	−1.41	−1.12
4.57	−1.74	−1.14
4.79	−1.98	−1.09
4.98	−2.17	−1.00
5.13	−2.32	−1.00
5.26	−2.43	−0.85
5.38	−2.54	−0.92
5.48	−2.63	−0.90

TDOF	**Err3**	**rate**
3.87	−1.00	−
4.28	−1.46	−1.12
4.57	−1.76	−1.03
4.79	−1.99	−1.04
4.98	−2.18	−1.00
5.13	−2.28	−0.67
5.26	−2.43	−1.15
5.38	−2.50	−0.58
5.48	−2.63	−1.3

To go far with our numerical studies, we plot and study the error curves ($Err2$ *and* $Err3$*) between the exact and numerical solutions corresponding to our problem. Figure 2 plots the comparison of the global error curves versus the total degree of*

TABLE 2. Adaptive method: rate of the error $Err2$ and $Err3$ with respect to the total degree of freedom in logarithmic scale.

TDOF	**Err2**	**rate**
3.87	-0.95	$-$
4.09	-1.63	-3.09
4.36	-1.92	-1.07
4.65	-2.43	-1.76
5.08	-2.85	-0.98
5.48	-3.19	-0.85

TDOF	**Err3**	**rate**
3.87	-1.00	-
4.09	-1.72	-3.27
4.36	-1.98	-0.96
4.65	-2.56	-2.00
5.08	-2.98	-0.98
5.48	-3.32	-0.85

freedom in logarithmic scale. We notice that the errors of the adaptive mesh method are smaller than those given by the uniform method.

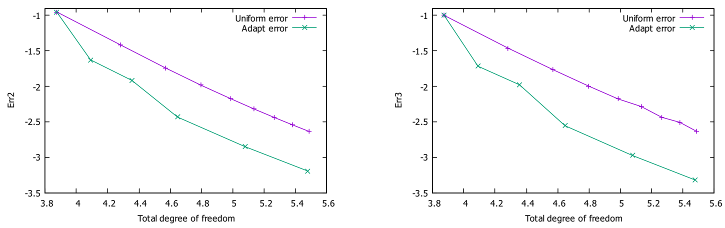

FIGURE 2. Comparison of the errors $Err2$ and $Err3$ with respect to the total degree of freedom in logarithmic scale.

In Table 3, we present the effectivity indices defined as :

$$EI2 = \frac{\eta_i^{(L)} + \eta_i^{(D)}}{\|\boldsymbol{u} - \boldsymbol{u}_h^{i+1}\|_{L^2(\Omega)} + ||\nabla(p - p_h^{i+1})||_{L^{3/2}(\Omega)} + ||C - C_h^{i+1}||_{H^1(\Omega)}}$$

and

$$EI3 = \frac{\eta_i^{(L)} + \eta_i^{(D)}}{\|\boldsymbol{u} - \boldsymbol{u}_h^{i+1}\|_{L^3(\Omega)} + ||\nabla(p - p_h^{i+1})||_{L^{3/2}(\Omega)} + ||C - C_h^{i+1}||_{H^1(\Omega)}}$$

with respect to the number of vertices during the refinement levels. Here $(\mathbf{u}_h^{i+1}, p_h^{i+1}, C_h^{i+1})$, $\eta_i^{(L)}$ *and* $\eta_i^{(D)}$ *are computed with the scheme* (V_{ahi}) *after convergence on the iterations* i *(by using the stopping criteria* (128)*). As indicated above, the effectivity indices* $EI2$ *and* $EI3$ *correspond respectively to the norms* $L^2(\Omega)^2$ *and* $L^3(\Omega)^2$*. We remark that the values of* $EI2$ *are between* 28.39 *and* 1.03 *while those of* $EI3$ *are between* 33.33 *and* 7.87.

TABLE 3. $EI2$ and $EI3$ with respect to the refinement levels.

Refinement Level	*initial*	*1*	*2*	*3*	*4*	*5*	*6*	*7*	*8*
Number of vertices	*441*	*485*	*1481*	*4323*	*15088*	*44940*	*152709*	*269821*	*422767*
EI2	*28.39*	*14.20*	*5.72*	*4.55*	*3.20*	*1.83*	*1.03*	*1.27*	*1.14*
EI3	*33.33*	*24.40*	*12.26*	*13.17*	*13.15*	*9.98*	*7.87*	*10.17*	*9.88*

Finally, Figure 3 show the map of the local effectivity index corresponding to $EI2$ *(with local norm* L^2 *for the velocity) given as*

$$EI2_K = \frac{\left((\eta_{K,i}^{(D_1)})^2 + (\eta_{K,i}^{(D_2)})^2 + (\eta_{K,i}^{(D_3)})^2\right)^{\frac{1}{2}}}{\|\boldsymbol{u} - \boldsymbol{u}_h^{i+1}\|_{L^2(K)} + ||\nabla(p - p_h^{i+1})||_{L^{3/2}(K)} + ||C - C_h^{i+1}||_{H^1(K)}}$$

on the entire mesh at the initial, first and second refinement levels.

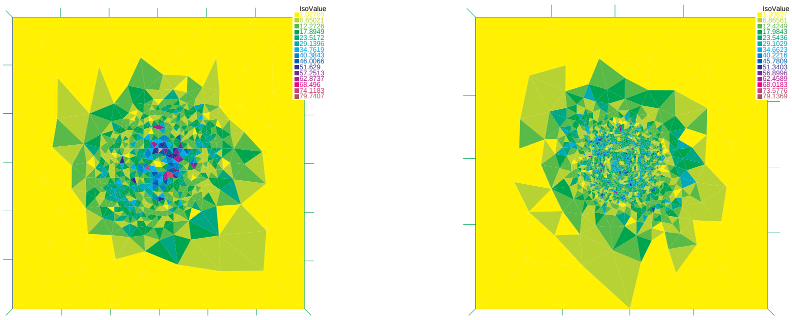

FIGURE 3. Map of the local effectivity index $EI2_K$ during the refinement levels (first (left) and second (right)).

5.2. Second test case (Driven cavity): *The driven cavity is a test of performance algorithms in fluid problems. It was used in several works and among them we cite* [36, 37, 6]*. In this subsection, we show numerical simulations corresponding to this test in order to study the a posteriori error estimates and the efficiency of the proposed method. We suppose that* $\Omega =]0,1[^2$, $K = I$, $\mu = r_0 = 1$, $\beta = 20$, $\gamma = 10$, $\mathbf{f}_0 = \mathbf{0}$, $\mathbf{f}_1(C) = (10C, 10C)$ *and* $g = 0$. *We complete the Darcy-Forchheimer equation with the boundary condition* $\mathbf{u} \cdot \mathbf{n} = 0$ *in* $\partial\Omega$, *and the convection-diffusion-reaction equation with the boundary condition* $C = 16x^2(x-1)^2$ *on the top* Γ_1 *of* Ω *and* $C = 0$ *on* $\partial\Omega \backslash \Gamma_1$. *Again, we consider an uniform initial mesh with* $N = 20$ *and we begin by showing comparisons between the uniform and adaptive methods corresponding to problem* (V_{ahi}). *Figure 4 presents the evolution of the mesh during the iterations. We can see that, from an iteration to another, the concentration of the refinement is on the complex vorticity regions and at the top boundary corresponding to* $y = 1$. *In Figures 5-(6), we consider the color velocity and concentration at*

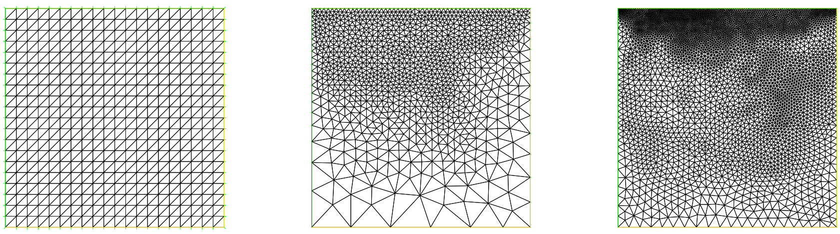

FIGURE 4. Evolution of the mesh during the refinement levels (initial, second and third).

the second refinement level. We remark that the solution is more important where the refinement of the mesh is concentrated (see Figure 4).
Now, we introduce the relative total errors (in $L^2(\Omega)^2$ *and* $L^2(\Omega)^3$ *for the velocity) to the indicator given by*

$$E_{tot2} = \frac{\eta_i^{(D)}}{\|\boldsymbol{u}_h^i\|_{L^2(\Omega)} + ||\nabla(p_h^i)||_{L^{3/2}(\Omega)} + ||C_h^i||_{H^1(\Omega)}}$$

and

$$E_{tot3} = \frac{\eta_i^{(D)}}{\|\boldsymbol{u}_h^i\|_{L^3(\Omega)} + ||\nabla(p_h^i)||_{L^{3/2}(\Omega)} + ||C_h^i||_{H^1(\Omega)}}$$

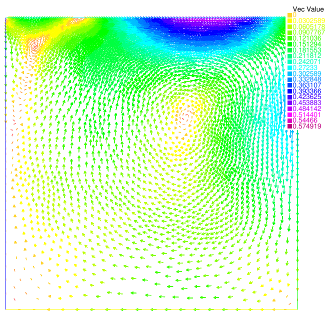

FIGURE 5. numerical velocity at the fourth refinement level.

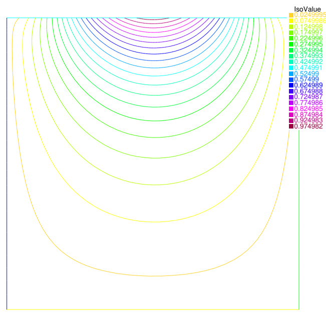

FIGURE 6. numerical concentration at the fourth refinement level.

where $\eta_i^{(D)}$ is computed after convergence on the iterations i (by using the stopping criteria (128)). In Figure 7, we plot the relative total errors E_{tot2} and E_{tot3} for the uniform and the adaptive methods. Note that E_{tot2} and E_{tot3} represent the global indicator errors (while $Err2$ and $Err3$ in the previous case represent the total errors between the exact and numerical solutions). We remark, like the first test case, that for the same total degree of freedom, the adaptive error is much smaller than the uniform error.

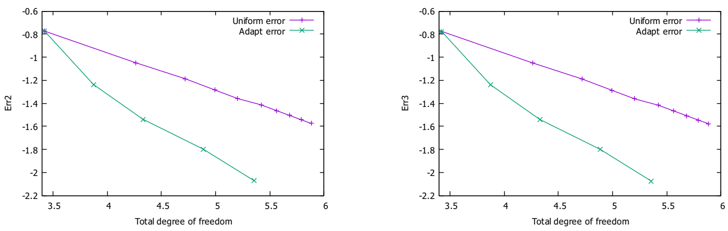

FIGURE 7. Comparison of the errors E_{tot2} and E_{tot3} with respect to the total degree of freedom in logarithmic scale.

Finally to end this section, we will show comparisons between the different parts of the discrete and iterative indicators for the adaptive method. We denote by: ($j = 1, 2, 3$ and $l = 1, 2$),

$$E_{tot2}^{D_j} = \frac{\eta_i^{(D_j)}}{\|\boldsymbol{u}_h^i\|_{L^2(\Omega)} + ||\nabla(p_h^i)||_{L^{3/2}(\Omega)} + ||C_h^i||_{H^1(\Omega)}}$$

$$(129) \qquad = \frac{\Big(\sum_{K\in\mathcal{T}_h} (\eta_{K,i}^{(D_j)})^2\Big)^{\frac{1}{2}}}{\|\boldsymbol{u}_h^i\|_{L^2(\Omega)} + ||\nabla(p_h^i)||_{L^{3/2}(\Omega)} + ||C_h^i||_{H^1(\Omega)}}$$

and

$$E_{tot2}^{L_l} = \frac{\eta_i^{(L_l)}}{\|\boldsymbol{u}_h^i\|_{L^2(\Omega)} + ||\nabla(p_h^i)||_{L^{3/2}(\Omega)} + ||C_h^i||_{H^1(\Omega)}}$$

$$(130) \qquad = \frac{\Big(\sum_{K\in\mathcal{T}_h} (\eta_{K,i}^{(L_l)})^2\Big)^{\frac{1}{2}}}{\|\boldsymbol{u}_h^i\|_{L^2(\Omega)} + ||\nabla(p_h^i)||_{L^{3/2}(\Omega)} + ||C_h^i||_{H^1(\Omega)}}$$

Table 4 show the values of $E^{L_l}_{tot2}$ *and* $E^{D_j}_{tot2}$ *during the refinement levels. We remark that the contribution of the indicators of discretization* $\eta^{D_j}_{tot2}, j = 1, 2, 3,$ *are of the same order while the indicators of linearization are very smaller as expected.*

TABLE 4. $E^{D_j}_{tot2}$ and $E^{L_l}_{tot2}$ in logaritmic scale with respect to the refinement levels.

Refinement Level	*initial*	*first*	*second*	*third*	*fourth*
Number of vertices	*441*	*485*	*1481*	*4323*	*15088*
$E^{D_1}_{tot2}$	*-1.09*	*-1.51*	*-1.82*	*-2.12*	*-2.43*
$E^{D_2}_{tot2}$	*-1.26*	*-1.62*	*-1.97*	*-2.28*	*-2.59*
$E^{D_3}_{tot2}$	*-0.86*	*-1.37*	*-1.65*	*-1.88*	*-2.14*
$E^{L_1}_{tot2}$	*-2.91*	*-3.36*	*-3.60*	*-3.95*	*-4.08*
$E^{L_2}_{tot2}$	*-4.23*	*-5.08*	*-5.66*	*-6.17*	*-6.45*

6. Conclusion

In this work, we introduced the variational formulation of the Darcy-Forchheimer problem coupled with the convection-diffusion-reaction equation. We discretized the problem by using finite element method. We then constructed indicators to evaluate the errors of the numerical approximation. Finally, we performed several numerical simulations where the indicators are used for mesh adaptation, confirming the efficiency of the adaptive methods.

Conflict of interest *The authors declare that they have no competing interests.*

References

[1] Adams J.A., Sobolev Spaces. Academic Press, New York, (1975).
[2] Alonso A., Error estimators for a mixed method, Numer. Math., 74(4), 385-395, (1996).
[3] Amaziane B., Bourgeois M. and El Fatini M., Adaptive Mesh Refinement for a Finite Volume Method for Flow and Transport of Radionuclides in Heterogeneous Porous Media. Oil and Gas Science and Technology - Rev. IFP Energies nouvelles, 69(4), pp. 687-699, (2014).
[4] Babuska I. and Rheinboldt W.C., Error estimates for adaptive finite element computations, SIAM J. Numer. Anal., 15(4), 736-754, (1978).
[5] Belhachmi, Z., Bernardi, C. and Deparis, Weighted Clément operator and application to the finite element discretization of the axisymmetric Stokes problem, Numer. Math., 105 (2), 105-217, (2006).
[6] Bernardi C., Dakroub J., Mansour G.& Sayah T., A posteriori analysis of iterative algorithms for Navier-Stokes Problem, ESIAM: Mathematical and Numerical Analysis, 50, 4, pp. 1035-1055, (2016).
[7] Bernardi C., Dib S., Girault V., Hecht F., Murat F. and Sayah T., Finite element method for Darcy's problem coupled with the heat equation. Numer. Math., 139 (2), pp. 315-348, (2018).
[8] Bernardi C. and Girault V., A local regularisation operation for triangular and quadrilateral finite elements. SIAM J. Numer. Anal.,, 35, pp. 1893-1916, (1998).
[9] Bernardi C., Maarouf S. and Yakoub D., Spectral discretization of Darcy's equations coupled with the heat equation. IMA Journal of Numerical Analysis, 36(3), pp. 1193-1216, (2015).
[10] Braess D. and Verfürth R., A posteriori error estimators for the Raviart-Thomas element, SIAM J. Numer. Anal., 33(6), 2431-2444, (1996).
[11] Carstensen C., Aposteriori error estimate for the mixed finite element method, Mathematics of Computation, 66(218), 465-476, (1997).
[12] Chalhoub N., Omnes P., Sayah T. and El Zahlaniyeh R., Full discretization of time dependent convection-diffusion-reaction equation coupled with the Darcy system. Calcolo, 57, 4, (2020).

[13] Chalhoub N., Omnes P., Sayah T. and El Zahlaniyeh R., A Posteriori error estimates for the time dependent convection-diffusion-reaction equation coupled with the Darcy system. Submitted to Calcolo, (2021).

[14] Ciarlet P. G., Basic error estimates for elliptic problems, In Handbook of Numerical Analysis, Vol. II, Handbook of Numerical Analysis, pages 17-351. North-Holland, Amsterdam, (1991).

[15] Clément P., Approximation by finite element functions using local regularization, RAIRO Anal. Numér. 9, R2,77-84, (1975).

[16] Dib D., Dib S. and Sayah T., New numerical studies for Darcy's problem coupled with the heat equation. Computational and Applied Mathematics, 39(1), (2020).

[17] Dib S., Girault V., Hecht F. and Sayah T., A posteriori error estimates for Darcy'a problem coupled with the heat equation, ESAIM: M2AN, 53(6), 2121-2159, (2019).

[18] El Alaoui L., Ern A.,Vohralík M., Guaranteed and robust a posteriori error estimates and balancing discretization and linearization errors for monotone nonlinear problems, Computable Methods in Applied Mechanics and Engineering 200, 2782-2795, (2011).

[19] Ern A. and Guermond J.L., Finite element quasi-interpolation and best approximation, ESAIM: Mathematical Modelling and Numerical Analysis, 51 (4), 1367-1385, (2017).

[20] Ern A., Vohralík M., Adaptive inexact Newton methods with a posteriori stopping criteria for nonlinear diffusion PDEs, SIAMJ. Sci. Comput. 35, 4, A1761-A1791, (2013).

[21] Fabrie P., Regularity of the solution of Darcy-Forchheimer's equation. Nonlinear Anal. Theory Methods, 13, 1025-1045, (1989).

[22] Forchheimer P., Wasserbewegung durch Boden, Z. Ver. Deutsh. Ing., 45, 1782-1788 (1901).

[23] Girault V. and Lions J.L., Two-grid finite-element schemes for the transient Navier-Stokes problem. M2AN Math. Model. Numer. Anal., 35(5), 945-980, (2001).

[24] Girault V. and Raviart P.A., Finite element methods for Navier-Stokes equations. Theory and Algorithms, SCM 5, Springer-Verlag, Berlin, (1986).

[25] Girault V. and Wheeler M.F., Numerical discretization of a Darcy-Forchheimer model, Numer. Math., 110(2), 161-198, (2008).

[26] Hecht F., New development in FreeFem++, Journal of Numerical Mathematics, 20, (2012), 251-266.

[27] Jose J.S, Lopez H. and Molina B. Comparison between different numerical discretizations for a Darcy-Forchheimer model, Electron. Trans. Numer. Anal., 34, 187-203, (2009).

[28] Lopez H., Molina B. and Salas J.J., An analysis of a mixed finite element method for a Darcy-Forchheimer model, Mathematical and Computer Modelling, 57, 2325-2338 (2013).

[29] Lovadina C. and Stenberg R., Energy norm a posteriori error estimates for mixed finite element methods, Mathematics of Computation, 75(256), 1659-1674, (2006).

[30] Nečas J., Les Méthodes directes en théorie des équations elliptiques. Masson, Paris, (1967).

[31] Neuman S.P., Theoretical derivation of Darcy's law, Acta Mech., 25(3), 153-170 (1977).

[32] Pan H. and Rui H., Mixed Element Method for Two-Dimensional Darcy-Forchheimer Model, J. Sci. Comput., 52, 563-587, (2012).

[33] Sayah T., Convergence analysis of numerical schemes for the Darcy-Forchheimer problem. Submitted , (2023).

[34] Sayah T., A posteriori error estimates for the Brinkman-Darcy-Forchheimer problem, Computational and Applied Mathematics, 40, 256, (2021).

[35] Sayah T., Semaan G and Triki F., A Posteriori error estimates for the Darcy-Forchheimer problem Computational Methods in Applied Mathematics. https://doi.org/10.1515/cmam-2022-0047,(2022).

[36] Sayah T., Semaan G., and Triki F., finite element methods for the Darcy-Forchheimer problem coupled with the convection-diffusion-reaction problem. ESAIM Math. Model. Numer. Anal., 55(6), 2643-2678, (2021).

[37] Schreiber R., Keller H. B, Driven cavity flows by efficient numerical techniques, Journal of Computational Physics, 49, 310-333, (1983).

[38] Scott L.R. and Zhang S., Finite element interpolation of nonsmooth functions satisfying boundary conditions. Math. Comp., 54, pp. 483-493, (1990).

[39] Shenoy A.V., Darcy-Forchheimer natural, forced and mixed convection heat transfer in non-Newtonian power-law fluid-saturated porous media. Transp Porous Med, 11, 219-241, (1993).

[40] Verfürth R. , A posteriori Error Estimation Techniques for finite Element Methods,,Numerical Mathematics And Scientific Computation, Oxford, (2013).

[41] Verfürth R., A review of A Posteriori error estimation and adaptive mesh-refinement techniques. Mathematics. Wiley and Teubner, New York, NY (1996).

[42] Whitaker S., Flow in porous media I: A theoretical derivation of Darcy's law, Transp. Porous Media, 1(1), 3-25 (1986).

Laboratoire Jean Kuntzmann, UMR CNRS 5224, Université Grenoble-Alpes, 700 Avenue Centrale, 38401 Saint-Martin-d'Hères, France.
E-mail: `faouzi.triki@univ-grenoble-alpes.fr`
URL: `https://membres-ljk.imag.fr/Faouzi.Triki/`

Unité de recherche "Mathématiques et Modélisation", CAR, Faculté des Sciences, Université Saint-Joseph de Beyrouth, B.P 11-514 Riad El Solh, Beyrouth 1107 2050, Liban.
E-mail: `toni.sayah@usj.edu.lb and georges.semaan2@net.usj.edu.lb`
URL: `https://www.usj.edu.lb/enseignants/?empid=639`